Journal of Materials Chemistry A

Accepted Manuscript

ROYAL SOCIETY OF CHEMISTRY

www.rsc.org/materialsA

Synthesis and stabilization of metal nanocatalysts for reduction reactions—A review

Huawen Hu, John H. Xin*, Hong Hu, Xiaowen Wang, Dagang Miao, Yang Liu

Nanotechnology Centre, Institute of Textiles and Clothing, The Hong Kong Polytechnic University, Hong Kong SAR 999077, China

E-mail: tcxinjh@polyu.edu.hk; Fax: +86-852-2766-6474

ToC Figure

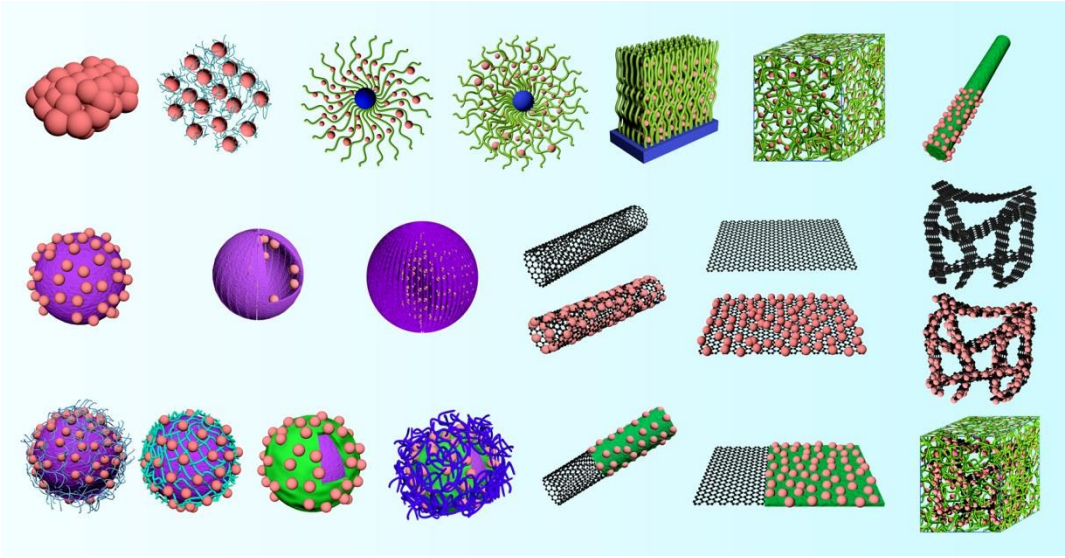

Review of stabilizing systems for metal nanocatalysts, such as surfactants, complexants, polymers, SiO_2, Fe_3O_4, graphene materials, and combined components thereof.

Abstract

Since the fast development of various chemical industries nowadays pose a serious threat to the environment in terms of leaving behind an increasing quantity of aromatic pollutants, to find an effective approach for handling the aromatic pollutants is of growing scientific and technological importance. Numerous research studies have attempted to address the environmental problem caused by aromatic pollutants with high attention to water-soluble aromatic dye and nitro compounds. In particular, the catalytic reduction of the dye and nitro compounds over metal-based catalysts have gained enormous interest in these years. However, review studies are rarely reported to summarize the contributions in this hot research area. Herein, we perform a review study to summarize these contributions, to discuss the existing problems, and to offer a guideline for future exploration; in the meanwhile, other methods for processing the aromatic pollutant are also briefly introduced. It is well known that the reduction reaction is highly dependent on catalysts since the reaction between an aromatic compound and a reducing agent either cannot take place or proceeds very slowly if without the assistance of a catalyst. As a result, this review article pays special attention to the widely reported metal-based catalysts for the reduction reaction. These catalysts are categorized into different groups on the basis of the stabilizing systems utilized for synthesis of the metal catalyst, mainly including surfactants/ligands, polymer supports, unmodified inorganic supports, functionalized inorganic supports, and organic combined with inorganic supports. As an important material in science and technology, especially in the field of catalysis due to its unique 2D structure and remarkable physicochemical properties, graphene used for supporting and stabilizing metal catalysts for the catalytic reduction reaction are specifically reviewed and summarized in the article. Finally, the remaining problems associated with the design and fabrication of cost-effective, efficient, and durable metal-based catalysts for the aromatic pollutant reduction are outlined.

Keywords: metal catalysts, stabilization, modification, composite catalysts, catalytic reduction reactions, dye and nitro compounds, graphene materials, binding sites

Content

1. Introduction

1.1. Impact of water-soluble aromatic pollutants on the environment

The rapid development of various industries is usually at the expense of over-exploiting and polluting the environment, especially the aquatic one, because a wide range of industries involve dealing with the wastewater that contains a high concentration of organic and inorganic pollutants. For instance, large quantities of aromatic pollutants, such as various kinds of dye and nitro compounds, are produced and manufactured at a daily rate in a wide range of industries, such as carpet, paper, leather, printing, pharmaceutical, paint and textile, which leaves a large amount of wastewater with a high content of residual pollutants even after the post-treatment by conventional methods. Most of the wastewater is released to the environment. Unfortunately, many kinds of aromatic contaminants dissolved in water can hardly be biodegraded or self-cleaned by the environment, which thus poses a direct and long-term toxic threat to amphibians and aquatic lives such as plants, micro-organisms and animals. This eventually threatens the lives on land including humans because of their heavy reliance on water and aquatic products in daily life, especially considering that some of the aromatic pollutants are carcinogenic and mutagenic in nature.[1] Even without toxicity, many water-soluble aromatic pollutants in trace quantities can cause water to be highly colorized, particularly the aromatic dye compounds. The colored wastewater can obstruct penetration of light and reduce oxygen dissolution, which diminishes the efficiency of photosynthesis in aquatic plants and hence disrupts the ecological balance in the aquatic ecosystem. Even worse, most water-soluble aromatic pollutants are difficult to remove or undergo a structure evolution because of their complex structure and synthetic origins that render

them recalcitrant,[2] which makes it rather difficult for remediation of the polluted aquatic environment and thereby causes persistent pollution.[3] For instance, as designed for resisting breakdown with time and exposure to water, sunlight, oxidizing agents and detergents such as soap, the synthetic dyes can hardly be tackled by conventional wastewater treatment processes.[4] In this context, highly efficient, economical, low-consuming, convenient and relatively green methods are needed to handle the increasing quantities of organic pollutants, especially the water-soluble aromatic ones.[3]

1.2. Approaches for dealing with water-soluble aromatic pollutants

1.2.1. Introduction

To effectively deal with the wastewater containing aromatic pollutants, many approaches have been explored including membrane separation, flocculation-coagulation, adsorption, oxidation or ozonation, photocatalytic degradation, chemical reduction with the catalyst assistance, and aerobic or anaerobic treatment. Membrane separation, including microfiltration, ultrafiltration, nanofiltration and reverse osmosis, is an effective method for direct separation of pollutants from wastewater. However, apart from the slow separation process, the special requirement of filtration setup and UHV condition makes it unsuitable for on-site processing. Even worse, organic pollutants can cause frequent clogging of the membrane pores, which causes the separation systems of limited use for the dye effluent treatment.[5] As for coagulation-flocculation-based methods, a huge amount of sludge can be generated because of the use of polyelectrolyte, ferrous salts, alum and/or lime, which thus brings about handling and disposal problems.[1] Biodegradation has also gained a great deal of attention due to its eco-friendly

characteristic, but the organic pollutant with complex aromatic molecular structure can hardly be biodegraded.[6] In addition, biodegradation is comparatively slow [7] and often not quite effective for treating the wastewater containing various types of dyes because most of the isolated algal, fungal or bacterial are dye specific.[1] Some conventional biochemical processes using active sludge have also been adopted to deal with wastewater, but a large amount of sludge could be left behind, causing disposal problems and increasing the operation cost. Furthermore, the traditional oxidation processes involving Fenton's reagent (H_2O_2/Fe^{2+}), H_2O_2, ozonization, etc., are not cost effective.[1]

The following three methods, namely adsorption, photocatalytic degradation and catalytic reduction, will be specifically introduced because they are widely employed currently to deal with the water-soluble aromatic pollutants, especially dye and nitro compounds. As the focus of the present review study, catalytic reduction method with the use of different kinds of catalysts will be described in more detail.

1.2.2. Adsorption

As an important technique for water purification, adsorption has attracted much attention in processing the organic effluent due to its easy operation without requirement of any equipment and chemicals other than an adsorbent, but the adsorption process is normally slow and cannot give a satisfactory result of decreasing the concentration of the aromatic pollutants in water before reaching saturation due to the limited adsorption capacity of the adsorbents.[8] This also reveals that, as for the highly colored wastewater, a complete decoloration can hardly be achieved only by adsorption processing. Additionally, the physical or chemical adsorption methods just transfer organic

contaminants from water to another phase and thus require further treatments (e.g., incineration or land filling) to destroy the end product,[9] which raises the processing costs and can easily cause secondary pollution. The post-treatment for regeneration of adsorbent materials is also difficult and expensive.[3]

In order to improve the adsorption efficiency, some powdery adsorbents are manufactured to be well dispersed in wastewater, which makes recycling very difficult even with the assistance of centrifugation. This indicates the difficulties in completely collecting the highly dispersed particles, which is likely to cause secondary environmental pollution.[10] For instance, graphene oxide (GO) powder has been well explored as an adsorbent for dealing with some aromatic dyes due to its large surface area and strong interactions with the dyes.[11-13] However, because of its strong hydrophilicity, the GO sheets can be stably dispersed in water, and ultrahigh centrifugation is usually required for recycling after each run of adsorption,[12] which is time-consuming and labor-intensive. Additionally, perhaps due to the difficulties and challenges in desorption of adsorbate from adsorbent, as well as to the unsatisfactory reusability, the desorption tests were even not attempted for many reported adsorbents.[14-18] Indeed, if without an effective desorption, the adsorption capacity will be lowered in a new using cycle, indicative of poor reusability.

There are some reports that have described the desorption processes such as those involving high-temperature burning,[19, 20] treatment with acid,[21] processing with strong basic solution and then with acid solution,[22] Soxhlet extraction,[23] and organic solvent processing.[24, 25] However, in addition to the additional operation cost generated by the arduous desorption process, the high temperatures involved not only cause a high energy

consumption, but also can have an adverse impact on the atmospheric environment since toxic gases might be generated during the burning process such as burning of the sulfur-containing aromatic pollutants. The volatile organic solvents used to induce the desorption are also environmentally undesirable.

1.2.3. Photocatalytic oxidation

Many studies have focused on the photocatalytic oxidation of water-soluble aromatic pollutants.[26-28] A variety of wide band gap semiconductor nanoparticles (NPs) and their hybrids/composites, especially TiO_2-based materials, have been extensively studied for the photocatalytic applications because they can enable the *in situ* generation of strong oxidizing intermediates to degrade persistent organic pollutants.[3] However, the use of the intensive light irradiation can make the photocatalytic process highly energy-consuming and thus limit the large-scale applications. Low quantum yields in most semiconductors might also hinder their practical applications.[29, 30] Moreover, apart from the time-consuming photochemical oxidation process,[1] it is of enormous challenge to handle the semiconductor nanopowder and to arrest the high surface energy-induced irreversible aggregation. To effectively prohibit the leaching of the NPs is also challenging since the NPs leaching is often observed,[31] which not only degrades the photocatalytic activity, but also might cause secondary environmental pollution; e.g., causing DNA damage in plants.[32]

It is worth pointing out that, owing to its enormous specific surface area,[33] minimal light blocking,[34] and zero conduction resistance for storing and transporting electrons,[35] graphene and its derivatives have been widely explored as the support for various

semiconductor photocatalysts, such as TiO_2,[36, 37] ZnO [38] and CdS.[39] Such hybridization of the semiconductor with graphene aims to enhance the migration efficiency of photo-induced electrons, to impede the recombination of photogenerated hole–electron pair, and/or to extend the light absorption to the visible light region.[40-43]

1.2.4. Catalytic reduction

The catalytic reduction of water-soluble aromatic pollutants over heterogeneous catalysts has received enormous interest due to its easy operation, high efficiency, clean processing, and low cost. In particular, catalytic reduction and decoloration of dye pollutants [33, 44-59] and transformation of poisonous nitro compounds to beneficial amino counterparts [47, 49, 56, 57, 60-68] have been widely reported. After the catalytic reduction processing, some aromatic pollutants with recalcitrant nature might be converted to readily biodegradable species,[57, 69] which thereby facilitates further degradation treatment if needed. Based on a unified reduction reaction model, such as reduction of an aromatic dye or nitro compound by $NaBH_4$, qualitative evaluation and comparison of the catalytic activities of different catalysts can also be achieved.[70]

However, on the other hand, most of the metal-based catalysts for the reduction reaction highly rely on the noble metals, such as Au, Ag, Pd and Pt,[71-78] indicating their high production cost and thus hindering their practical applications.[79] Having a high tendency to minimize their high surface energy, the nanostructured metal-based catalysts can also undergo an easy aggregation if without effective protection and stabilization of the nanocatalysts,[59, 71, 80] which can lead to degradation of their catalytic activities and hence reduce their lifetime.[59, 81-83] For example, the aggregation of Ag–Au bimetallic NPs

was found to occur without protection by a triblock copolymer surfactant, whereas the surfactant stabilized-bimetallic NPs could be colloidally stable at room temperature for a period of several weeks.[80] Agglomeration of the $Fe_3[Co(CN)_6]_2$ particles was also observed if without the PVP protection.[79] Furthermore, without stabilization by silica spheres, the colloidal metal NPs were found to flocculate during a catalytic reaction,[45] which could lead to a gradual loss of their catalytic activity and selectivity.[84]

To arrest the aggregation of metal NPs, a range of organic surfactants and ligands have been explored to cap or passivate the active crystallographic plans of metal NPs, such as dodecyl sulphate (SDS) [59, 85] and cetyltrimethyl ammonium bromide (CTAB),[59] 16-mercaptohexadecanoic acid,[86] polyvinylpyrrolidone (PVP),[87] diethylenglycol combined with PVP,[88] polyvinyl alcohol (PVA) [89] and polyethylene glycol.[90] Nevertheless, even though the dispersion state and stability of the metal NPs can be improved, and the controllable synthesis of various shaped metal NPs is also likely to be achieved,[91] the capping and passivation of the active facets of metal NPs can cause the degradation of the catalytic properties,[87, 92] especially for the stabilizers or capping agents with strong coordination properties.[93] For example, the catalytic reduction of 4-nitrophenol (4NP) over hexagonal boron nitridesheets/Ag composites was found to be blocked by adding PVP to the reaction system.[94] It was also observed that the catalytic effect of a GO/Ag NPs hybrid catalyst on the 4NP reduction almost disappeared when a little amount of PVP was added, and the reduction reaction efficiency turned out to be close to that in the reaction system without a catalyst.[87] In addition, the presence of CTAB or SDS in the catalytic reaction solution could impede the catalytic reduction of dye compounds, as caused either by the competition of CTAB with the dye molecules to

adsorb onto the surfaces of Au NPs, or by the formation of SDS–dye complex that hindered the physical contact of dyes with the Au catalyst surfaces.[44] Addition of cationic (CTAB), anionic (SDS) or nonionic (Triton X-100) surfactant could also bring about an obvious decrease in the reaction rate of the reduction of an azo dye over a Fe_3O_4@polyaniline (PANI)@Au catalyst.[7] Likewise, the presence of Triton X-100, SDS or CTAB could depress the catalytic activity of Ag NPs to some extent, as caused by competition between the surfactant and reactants for interaction with the Ag catalyst.[45] Furthermore, a larger decrease in catalytic reaction rate was observed when a dye and surfactant carry the same charge as compared to the case of those with the opposite charge.[95] Therefore, these results corroborate that ligands and surfactants can poison or deactivate the metal catalyst as a consequence of interacting with the catalyst or strongly packing around it, thus adversely affecting the accessibility of catalysant/substrate molecules to the catalyst surfaces.[96]

In addition to using organic surfactants or ligands to impede the aggregation of metal NPs, much effort has also been devoted to dispersing and immobilizing the metal nanocatalysts onto various carrier systems, such as Kapok fiber,[46] chitosan–grafted poly(acrylic acid) (PAA) hydrogel,[48] ferrocenyl–based honeycomb oligomer film,[55] PAA–amidodiol hydrogels,[58] tree–like brushes,[97] core–shell microgels,[98, 99] spherical polyelectrolyte brushes,[70] tree–like brush entrapped in PVA composite hydrogel,[100] PVA hydrogel,[101] polyamidoamine dendrimer [102] and polyelectrolyte/dendrimer multilayer films.[103] In most of the cases studied, the carrier systems only provide suitable support for the metal NPs to prevent them from aggregation and to facilitate catalyst recycling,[104] without making an additional contribution to the catalytic performance of the resulting

composite catalyst; e.g., to enhance the electron mobility. Moreover, some carrier systems cannot even effectively stabilize the metal catalysts. Specifically, if the polymer network such as hydrogel, brush and dendrimer are in a highly swollen state, the confining force on the encapsulated metal NPs will be largely weakened, which indicates that easy aggregation of the NPs can take place, and release of the NPs from the swollen polymer network can also occur. On the other hand, in order to highly stabilize the metal NPs, the polymer network density should be sufficiently high. However, this not only inhibits the diffusion of the reactant molecules into the network, but also makes the soft polymer chains closely pack around the surfaces of the metal NPs, which can lead to a loss of catalytic activity.[45] For example, it was reported that the dendrimer molecules at a higher concentration were likely to adsorb onto the Au surfaces, which could interfere with the diffusion of 4NP to the surfaces of the Au NPs and thus lower the catalytic efficiency.[105] Conversely, decreasing the generation and/or concentration of dendrimers could accelerate the catalytic reduction of 4NP.[106] However, it was also observed that the insufficient immobilization effect on the metal NPs formed initially within a conventional spherical brush allowed the NPs to have enough diffusional mobility, leading to their coagulation.[97]

In these contexts, using rigid inorganic materials as the carrier system becomes more desirable with regard to avoiding the above-mentioned problems associated with the organic surfactants, ligands and polymer supports. Specifically, large quantities of clean surfaces of the metal NPs deposited on the inorganic substrate can be exposed and accessed by the catalysant molecules. In addition, inorganic materials normally possesses higher thermal stability and chemical resistance as compared to organic ones,[49, 81, 107]

making the resulting catalyst applicable in harsh environments. This can also explain why organic matrices are usually filled with inorganic additives to fabricate the high-performance composite materials with improved mechanical, thermal and other properties.[108-115] Furthermore, apart from dispersing and immobilizing metal catalyst, some inorganic carrier systems can make additional contributions to the catalytic reactions, in contrast to most support materials with inert properties. For instance, a carbon nanofiber could help deliver electrons for its hybrid with Ag NPs to accelerate the catalytic reduction of 4NP.[61] Such a contribution can also be obtained from carbon nanotubes (CNTs) and graphene sheets (GSs) if used as the catalyst support due to their sp^2-conjugated structures [33, 49, 116] that are able to store and shuttle electrons [117] and can also act as an electron-donating source to reduce a precious metal ion.[86] It has also been hypothesized that the empty π-orbitals in the CTNs and GSs can overlap with the filled metal d-orbitals, which possibly affords unique electronic and catalytic properties to the resulting metal-carbon composites.[92, 118]

Among the inorganic support materials, graphene occupies a particular position owing to its following merits: (i) the huge specific surface area makes graphene highly desirable as a 2D catalyst support, with both the top and bottom surfaces that can be exploited, which is superior to the CNT with only accessible outer surface; (ii) graphene π system, i.e., sp^2-hybridized carbon network, could store and shuttle electrons and enable the adsorption of aromatic molecules via π-π stacking interactions. The capability of storing and shuttling electrons has been schematically illustrated in Fig. 1.[117] The electrons from photoexcited semiconductor NPs can first be transferred into GO for its reduction to reduced graphene oxide (RGO), and then the stored electrons in RGO can be

shuttled to precious metal ions for their reduction to metal NPs; (iii) graphene can be easily functionalized and modified using GO as a precursor through a simple and cost-effective solution route;[119, 120] (iv) oxygen functionalities and structural defects on graphene surfaces can serve as the nucleation and binding sites for metal NPs;[121] (v) upon incorporating with graphene, metal nanocatalysts can be more easily recycled,[107] thereby reducing the probability of releasing the toxic metal NPs into the environment; (vi) the size and density of the metal NPs deposited on the enormous surfaces of graphene materials can be easily and finely tuned, which also indicates the tunable catalytic performance of the resulting composite catalyst.

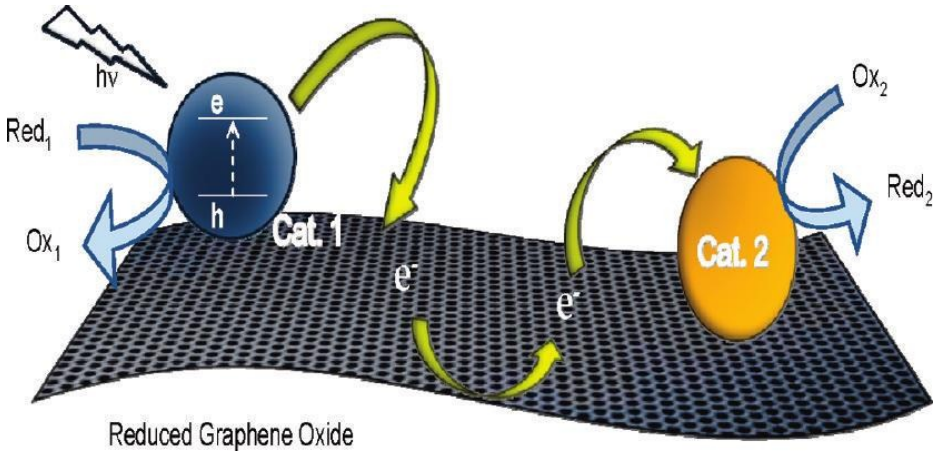

Fig. 1 RGO as 2D conducting support to carry out selective catalysis at different sites.[117]

However, on the other hand, pure inorganic supports, such as pristine graphene without modification or functionalization generally cannot effectively stabilize the metal NPs due to a lack of binding sites. Even though metal nanocrystals can be grown and immobilized on GO sheets because a high abundance of oxygen groups and structural defects present on GO surfaces are able to serve as nucleation sites,[86] and also capable of interacting with metal NPs through physisorption, electrostatic binding or charge-transfer

interactions,[122] these nanocrystals deposited on GO surfaces are not stable and can be varied with the change of the labile oxygen groups that can undergo an easy reduction, especially in reductive and high-temperature environments. For instance, the reduction of the nucleation sites on GO surfaces has been found to induce the aggregation of metal NPs and formation of larger agglomerates.[86, 123] In these regards, it is highly desirable to integrate both organic and inorganic structures for well supporting and stabilizing metal catalysts, and in the meanwhile for generating high catalytic efficiencies in the final composite catalysts. This is because the heterogeneous catalysts with multiple integrated functional components can combine the advantages of different components to overcome the drawbacks of the single component-stabilized metal catalysts.[124, 125] However, effective integration of different functional components into a high-performance composite catalyst usually involves a complex and long process with the need of multistep procedures and many kinds of hazardous chemicals as the raw materials, which can raise the production cost and easily cause an environmental problem, thus limiting large-scale applications. As a result, more effort needs to be invested in exploring convenient, green and efficient routes to synthesis of high-performance multicomponent composite catalysts for the reduction reactions, especially from the viewpoint of practical applications.

After the general introduction and analysis of the different stabilizing systems used for preparing the metal-based catalysts for the reduction reactions, the following section presents the specific case studies of the metal-based catalysts that are categorized into different groups based on the stabilizing systems employed.

2. Literature review and discussion

2.1. Naked metal catalysts

Few reports can be found on exploration of naked metal catalysts for the reduction of aromatic pollutants, which can be an indication of the necessity of using a stabilizer or carrier system for producing an efficient and durable catalyst. It has been reported that naked, unsupported metal NPs tend to aggregate due to their high surface energy and result in a decrease of the catalytic activity over time.[126]

Naked Ni particles were reported for catalysis of the 4NP reduction.[127] Such nickel particles were prepared in an aqueous solution by a chemical reduction method. As expected, the as-prepared naked Ni NPs were prone to aggregation, as verified by large agglomerates observed in the scanning electron microscopy (SEM) image (Fig. 2). In addition, partial sintering of the prepared nickel catalyst could further deactivate the catalyst. This might be because such sintering can lead to heavier aggregation and even fusion of the nickel particles into a bulk form, causing a great loss of the accessible catalyst surfaces along with the active low-coordination sites such as edges and corners and hence bringing about the depressed catalytic activity. Similarly, Ni particles were also prepared as a catalyst for the 4NP hydrogenation,[128] using the same preparation method presented in the Ref.[127] The catalytic activity of the as-prepared nickel particles showed a strong dependence on the apparent pH of the initial solution.

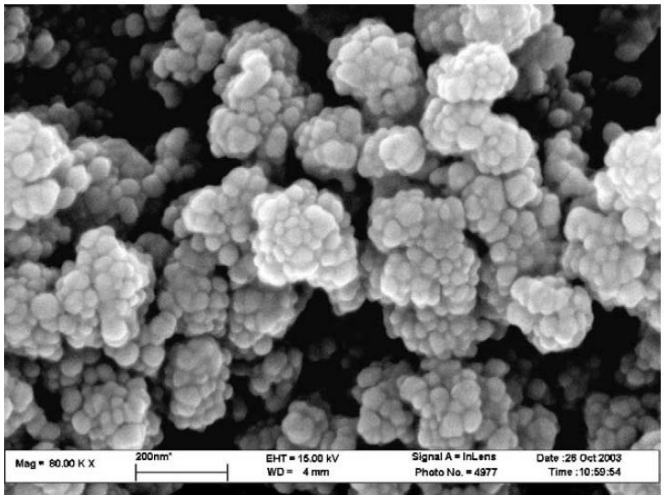

Fig. 2 SEM image of nickel catalyst.[127]

Based on a galvanic replacement reaction method, Ag dendrite-based Au-Ag bimetallic nanostructure was also fabricated as a catalyst for the 4NP reduction.[129] Following this work, Pd-Ag bimetallic dendrites were further synthesized as a catalyst for the 4NP reduction.[130] It was found that the Pd-Ag dendrite performed better than the Au-Ag counterpart in the catalytic reduction reaction. However, regardless of the stability and durability of the naked bimetallic nanostructures, the preparation process can leave behind much effluent and sludge containing metallic contaminants such as Cu^{2+} in the first step and AgCl in the second step.

Both *in situ* formed Ag NPs- and full grown Ag NPs were also explored for the catalytic reduction of aromatic compounds.[131] Different kinds of reducing agents were used for the catalytic reactions, including $NaBH_4$, hydrazine, alkaline solution of ascorbic acid, and molecular hydrogen. Only $NaBH_4$ was capable of effectively reducing a series of nitro compounds over the Ag catalysts. However, catalyst durability is not examined in the work although it correlates closely with the catalyst life time. Furthermore, a series of

monometallic and multi-metallic nanosponges were fabricated for the catalytic reduction of Congo red dye and 4NP.[132] However, a recycling experiment is not considered despite its importance in catalysis. More information about naked metal NPs as catalysts for the reduction reactions is summarized in Table 1.

In summary, some considerations given to the naked metal-based nanocatalysts are described as follows: (i) without protection, surface passivation or immobilization onto a support system, metal NPs can suffer from an easy aggregation owing to their high surface energy and strong van der Walls interactions, which will cause instability and rapid decay of catalytic activity;[133] (ii) without a carrier system, recovery of the powdery nanocatalysts will be difficult, as tedious and costly separation process is normally required, limiting their widespread application;[83] (iii) the difficulties in recycling will also present a threat to the environment due to the toxicity of metal NPs.[134]

Table 1 Summary of the reduction reactions catalyzed by naked metal catalysts.

Metal catalyst	Stabilizer or carrier system	Reductant 1	Catalysant/substrate	Reductant 2	Solvent	Reaction condition	Ref.
Ni	-	hydrazine hydrate	4NP	molecular hydrogen	ethanol	82-110 ^{o}C, violent stirring	127
Ni	-	hydrazine hydrate	4NP	molecular hydrogen	ethanol–water mixture (v/v: 143/20)	pH: 1.5–9.5, 102 ^{o}C, stirring	128
Pd-Ag	-	galvanic replacement reaction	4NP	$NaBH_4$	water	room temperature	130
Au-Ag	-	galvanic replacement reaction	4NP	$NaBH_4$	water	room temperature	129
Ag	-	$NaBH_4$, hydrazine, ascorbate anion, or molecular hydrogen	4-NP, 2-nitrophenol, 4-nitroaniline	$NaBH_4$	water	room temperature	131

Note:

Reductant 1----used for conversion of metal ions to the corresponding zero-valent metals.

Reductant 2, Solvent and Reaction condition----used for catalytic reduction reactions.

2.2. Organic surfactant and/or ligand-stabilized metal catalysts

Using organic surfactant and/or ligand to synthesize metal catalysts is a conventional method, and this subsection will summarize the typical work devoted to preparing the organic surfactant and/or ligand-stabilized metal catalysts for the reduction of aromatic pollutants.

Submicron-sized Ag particles were synthesized and protected with ethylenediaminetetraacetic acid (EDTA) as both reducing and chelating agents through a hydrothermal process.[135] Only moderate catalytic efficiency was achieved in the resulting Ag catalysts for the 4NP reduction, which is probably attributed to the presence of capping agent EDTA on the Ag surfaces and to the large size of the Ag particles that is beyond the nano-sized range. In addition, different complexants including ethylene diamine, triethylenetetramine and EDTA were used to stabilize corresponding nanostructured Co, Ni and CoNi alloy films for catalysis of the 4NP reduction.[83] Various anionic complexing ligands were also explored to both reduce silver ions and stabilize Ag NPs for the catalytic reduction of o-nitroaniline.[136] It was found that the rate constant of the catalytic reaction over these complexing ligands-stabilized metal NPs was dependent on the available clean surface area of the stabilized metal NPs. This also elucidates that occupying the metal surface by the ligand can reduce the clean surface area and hence cause the degradation of the catalytic properties.

A nanoporous Au–Pd bimetallic foam was prepared and stabilized using dextran as both a surfactant and reducing agent through a mild hydrothermal process.[65] The as-prepared bimetallic foams were then used to catalyze the 2-nitrophenol reduction, but the

important durability of the catalyst was not investigated. Using PVP as a stabilizing agent, the colloids of monometallic Pd and bimetallic Pd-based alloy including Pd-M (M=Ag, Au, Cu, Ni, and Pt) were also produced under γ-ray irradiation.[66] However, the presence of dextran or PVP can poison the catalyst and lower the catalytic activity.

In order to optimize the catalytic activity, shape-controlled synthesis of nanostructured metal catalysts using the surfactant and/or ligand has received much interest. For example, differently shaped Au NPs were synthesized and stabilized by surfactants using a seed-mediated growth process.[59] Among all the as-synthesized Au NPs with different shapes, the dendrimer-shaped Au NPs possessed the highest catalytic activity for the reduction of an azo dye, in this case sudan-1, to the product, namely 1-amino-2-naphthol and aniline. Au NPs with diverse shapes were also prepared under microwave irradiation,[90] and the Au nanorods exhibited the highest activity in catalyzing the reduction of 2,4,6-trinitrophenol to 2,4,6-triaminophenol. In addition, Au nanospheres, nanorods and nanoprisms were prepared for the catalytic reduction of different aromatic nitro compounds to the corresponding amino derivatives,[137] and the Au nanospheres performed the best in the catalytic reduction of different aromatic nitro compounds to the corresponding amino derivatives. Similarly, spherical, flower-like, and cubical rhodium (Rh) nanocatalysts were also fabricated,[138] and the Rh nanocubes outperformed other shaped Rh NPs in the catalytic reduction of different aromatic nitro compounds. Following this report,[138] Iridium (Ir) nanocatalysts with variable shapes were further synthesized,[139] and needle-shaped Ir NPs were superior to sphere-, chain- and flake-like Ir NPs in the catalytic reduction of dye compounds including MB, RhB, and Rose Bengal. However, it is worth noting that the shape of the metal NPs can change and has a

tendency to assume the most stable (spherical) shape during the catalytic reaction by considering that the surface energy of the spherical shape is the lowest,[140] which thereby reveals that the shape effect might be gradually attenuated and eventually vanished during a long-term usage.

Recently, a multivariate analysis was used to optimize the reactant concentration in order to synthesize a PVP-stabilized Ag nanocatalyst with the optimal catalytic properties based on the catalytic reduction of 4NP by $NaBH_4$ as a model reaction.[93] The best synthetic conditions were thereby *in situ* selected to produce the optimal PVP-Ag catalyst. Subsequently, the kinetics of the catalytic reaction was investigated in the reduction of different aromatic nitro compounds, with the results revealing that adsorption of the nitro compounds had a crucial effect on the performance of the Ag catalyst. As a result, the nature and amount of the stabilizer PVP used in the preparation of the Ag catalyst correlated closely with the catalyst performance. It was also found that the nitro compounds with an electron-withdrawing substituent were more catalytically favored. Following this work, a Ag nanocatalyst stabilized by an oligosaccharide-based amphiphiles with terminal carboxyl groups was further prepared.[141] The carboxyl groups could coordinate the surfaces of Ag NPs and thus made the Ag NPs stable. To optimize the stabilization of the Ag NPs with a view to obtaining long-term storage, the multivariate approach was also employed.

With a triblock copolymer Pluronic F127 as a surfactant, bimetallic Ag-Au NPs were produced and stabilized through a modified galvanic replacement reaction.[80] It was found that the bimetallic NPs had ~2 — 10-fold higher catalytic activity in the 4NP reduction than typically reported for monometallic Au and Ag NPs of comparable sizes.

The partially hollow bimetallic NPs exhibited the highest activity among the fabricated catalysts. However, the triblock copolymer seems to form a thick layer on the surfaces of NPs, indicative of the added barrier to the 4NP molecules of passing through the thick layer during the catalytic reaction. The important recycling experiment is also not considered.

The fruit juice of Punica granatum was also exploited to synthesize and stabilize the Au and Ag NPs for the catalytic reduction of different kinds of dye compounds.[142] The protein present in the juice was surmised as both reducing and stabilizing agents, and the phenolic hydroxyls were suggested as the specific reducing agent for conversion of the metal ions to metal NPs. The latex of Jatropha gossypifolia was also employed to prepare and stabilize Ag NPs, and the latex metabolites such as proteins, polyphenols, alkaloids, saponins and terpenes could both act as reducing agents and confer the Ag NPs with stability by capping around them.[143] Furthermore, erythromycin was used as both reducing and capping agents to fabricate and stabilize Ag NPs for the catalytic reduction of differently charged dyes including MB (cationic), eosin B (anionic) and rose bengal (neutral).[144] However, the strong capping effect of the juice, latex or erythromycin on the Au or Ag NPs was likely to lower the catalytic activity for the dye compound reduction. More information about the work devoted to fabrication of metal-based catalysts stabilized by surfactant and/or ligand is summarized in Table 2.

To conclude, the presence of surfactants and/or complexing ligands can strongly attach to the metal catalyst surfaces, especially for those with strong coordination capability,[93] which thus blocks the access of substrate/catalystant molecules to the catalyst surfaces and consequently lowers the catalytic activity. In addition, it is usually

difficult to recover/regenerate the surfactant or complexant-stabilized metal NPs due to their nanoscale size and good dispersion state in the catalytic reaction solution. Even with the assistance of high-speed centrifugation, some unseparated metal NPs can still exist in the supernatant. The residual nanomaterials are most likely to cause a side effect on the environment.[25]

Table 2 Summary of the catalytic reduction reactions over surfactant or ligand-stabilized metal nanocatalysts.

Metal catalyst	Stabilizer or Carrier System	Reductant 1	Catalysant/substrate	Reductant 2	Solvent	Reaction Condition	Ref.
Ag, Au, Pd, Pt, Co, Ni, Cu, Ag–Au, Ag–Pd, Ag–Pt, Pd–Pt, Ag–Au–Pd	glycerol (might be more like a solvent or a reducing agent than a stabilizer)	hydrazine	Congo red, 4NP	$NaBH_4$	water	room temperature	132
Rh	CTAB	2,7-DHN, under UV photoirradiation	aromatic nitro compounds	$NaBH_4$	water	room temperature	138
Ir	CTAB	2,7-DHN, under UV irradiation	MB, RhB, Rose Bengal	$NaBH_4$	water	room temperature	139
Au	trisodium citrate (Au seed), CTAB (Au nanosphere, nanorod and nanoprism)	$NaBH_4$ (Au seed), ascorbic acid (Au nanosphere and nanorod), 2,7-DHN (Au nanoprism)	aromatic nitro compounds	$NaBH_4$	water	room temperature	137
Ag	EDTA	EDTA, hydrothermal reaction at 150 ^oC	4NP	$NaBH_4$	water	22 ^oC, stirring	135
Ag	a range of anionic complexing ligands including EDTA, HEDTA, NTA, TTHA and IDA	EDTA, HEDTA, NTA, TTHA and IDA, under alkaline condition	o-nitroaniline	$NaBH_4$	water	vigorous stirring, 25 ^oC	136
Au–Pd	dextran	hydrothermal process (100 ^oC) in the presence of dextran	2-nitrophenol	KBH_4	water	room temperature	65
Au	SDS (for seed preparation), CTAB (for growth)	$NaBH_4$ (for seed preparation), ascorbic acid (for growth)	sudan-1 (azo dye)	$NaBH_4$	mixture of ethanol and water	room temperature, stirring	59
Pd, Pd-M (M = Ag, Au, Cu, Ni and Pt)	PVP	γ-ray irradiation	4NP	$NaBH_4$	water	room temperature	66
Ag	PVP	$NaBH_4$	different nitroaromatic compounds	$NaBH_4$	water	15 °C	93

Ag	erythromycin	erythromycin	MB, eosin B, Rose Bengal	$NaBH_4$	water	room temperature	144
Au or Ag	proteins present in the fruit juice of Punica granatum	fruit juice of Punica granatum (phenolic hydroxyls)	MB, Methyl Orange, Eosin Y	$NaBH_4$	water	room temperature, stirring	142
Ag	nonionic surfactant Igepal CO-520	hydrophilic polyethylene oxide groups of Igepal CO-520, hydrazine	MB	$NaBH_4$	water	room temperature	145
Cu, Ag	cetyltrimethylammonium chloride, PVP	ascorbic acid, hydrothermal at 120 ^oC, galvanic replacement reaction	4NP	$NaBH_4$	water	room temperature	146
Ag–Au	triblock copolymer surfactant Pluronic F127	maltose, trisodium citrate, galvanic replacement reaction	4NP	$NaBH_4$	water	pH 9 temperatures in the range of 25 to 45 ^oC	80
Co, Ni and CoNi alloy films supported on Cu foil	ethylene diamine, triethylenetetramine, EDTA	hydrazine hydrate, hydrothermal at 100 ^oC	4NP	$NaBH_4$	water	25 ^oC	83
Au–Ag	fruit juice of pomegranate	fruit juice of pomegranate	2-, 3-, 4-nitrophenols, methyl orange dye	$NaBH_4$	water	room temperature, stirring	147
Ag	latex of Jatropha gossypifolia (latex metabolites such as proteins, polyphenols, alkaloids, saponins, and terpenes)	latex of Jatropha gossypifolia (latex metabolites such as proteins, polyphenols, alkaloids, saponins, and terpenes)	MB, eosin B	latex metabolites	water	room temperature	143
Ag	amoxicillin antibiotic	amoxicillin antibiotic	cefdinir, cefditoren, ceftriaxone sodium, doxycycline, cefixime	$NaBH_4$	water	room temperature	148
Ag	ceftriaxone standard (Antibiotic)	ceftriaxone standard (Antibiotic)	4-nitro-1,3-Phenylene diamine, 6-methyl-2-nitroanilline, 4-methyle-2-nitroanilline	$NaBH_4$	water	room temperature	149
Ni	L-threonine	$NaBH_4$	Congo red	$NaBH_4$	water	room temperature	9
Cu	olive oil	olive oil, heated to 270 ^oC under N_2 protection	MB, RhB, methyl orange, Congo red	$NaBH_4$	water	room temperature	150
Ag	Oligosaccharide-based amphiphiles functionalized with terminal carboxyl groups	$NaBH_4$	4NP	$NaBH_4$	water or water/ethanol mixtures	25.0 °C	141
Au	hydroxypropyl methyl cellulose or polyethylene glycol (M.W. 200, 400 and 600)	ethylene glycol, polyethylene glycol (under microwave irradiation)	2,4,6-trinitrophenol	$NaBH_4$	water	room temperature, stirring	90
Ag	lithium dodecyl sulphate	lithium dodecyl sulphate	MB, eosin	$NaBH_4$	water (for MB and eosin) or micellar solution with surfactant (for MB)	room temperature	95

2.3. Organic polymer-supported metal catalysts

Polymer hydrogels have been widely explored as carrier systems for metal NPs owing to their functionalities and porous network structures. They can also be facilely prepared by different polymerization methods, such as free-radical [49] and ionic [151] polymerizations, based on inexpensive and convenient solution route. For example, a core-shell microgel consisting of a solid polystyrene (PS) core and a shell of cross-linked poly(N-isopropylacrylamide) (PNIPA) was used to stabilize a Pd nanocatalyst.[98] The microgel-based system was also quantitatively compared with a spherical polyelectrolyte brush-based one being composed of the solid PS core and long chains of poly((2-methylpropenoyloxyethyl) trimethylammonium chloride) as a shell. It was found that the catalytic activity of the polyelectrolyte brush-based catalyst was much higher than that of the microgel-stabilized one, which could be attributed to the different diffusional barriers existing in these stabilizing systems. Similarly, a bottlebrush polymer densely grafted on a solid PS core was specifically explored as a carrier system for Ag NPs.[97] However, the preparation process is sophisticated, which can cause difficulties in operation and high cost in terms of time, manpower and raw materials, thus limiting large-scale practical applications.

A poly(methacrylic acid) microgel was also employed as a carrier system to first adsorb the metal ions by means of electrostatic interactions and then *in situ* reduce the adsorbed metal ions to the corresponding metal NPs.[152] Likewise, a modified poly(4-vinylpyridine) cryogel was reported to adsorb metal ions, followed by *in situ* reduction treatment to produce a composite catalyst for the reduction of MB dye and 4NP.[153] In addition, the fibrillar network of poly(acrylic acid)–based hydrogel was used to entrap Ag

NPs using amidodiol as both cross-linking and reducing agents.[58] The prepared hydrogel-immobilized Ag NPs was then applied to the catalytic reduction of cationic dyes including rhodamine 6G (R6G), MB and crystal violet. It was found that pH and temperature had a significant effect on the catalytic reaction.

Calcium alginate (CA) gel beads were used as both reducing and stabilizing agents to synthesize Ag and Au NPs.[154] The as-prepared CA-stabilized Ag nanocatalyst were more efficient in the catalytic conversion of 4NP to 4AP than the Au counterpart, so the authors speculated that metallic Ag could be a better catalyst than Au in this catalytic reduction reaction. In addition, it was presumed that the loading amount of the Ag NPs on alginate (or the surface coverage with Ag NPs) could be more favorable for the catalytic reaction as compared to that of the Au NPs. Similarly, Ag NPs-imbedded hydrogel beads were prepared for catalysis of the 4NP reduction.[151] It was observed that the gelation reaction could be induced directly by Ag^{+} ions alone through ionic polymerization, while Ba^{2+} ions played a crucial role in maintaining the structural stability of the formed hydrogel beads during the catalytic reaction. Nevertheless, such composite beads seem not durable because an apparent loss in catalytic activity occurs only after 3 circles of repeated usage. Such a loss might be attributed to the aggregation of the Ag NPs within the hydrogel beads or release of NPs from the beads during the reusability test, revealing that Ag NPs could not be highly stabilized only by the confining effect of the hydrogel network.

Polymer dendrimers are also popular choices as stabilizing systems for metal catalysts. For example, poly(amidoammine) (PAMAM) and poly(propyleneimine) (PPI) dendrimers were used to stabilize Au NPs for catalysis of the 4NP reduction.[105] As

mainly controlled by the 4NP diffusion, the reduction rate constant was decreased with increasing dendrimer concentrations as a consequence of an increased amount of the dendrimer that occupied more clean surfaces of Au NPs and hence of an increased diffusion barrier generated between 4NP and Au nanocatalyst. In addition, PAMAM and PPI dendrimers were used to stabilize Ag, Pt and Pd NPs.[155] It was found that the catalytic reduction rate constants for all the investigated systems decreased with increasing dendrimer concentration. PAMAM and PPI dendrimers with surface amino groups were also investigated to prepare and stabilize Au NPs-based composite catalyst by laser irradiation reduction instead of by a chemical reduction method.[106] The average diameter of the resulting Au NPs decreased with irradiation time. It was also inferred that the dendrimers were adsorbed on the surfaces of the NPs as a monolayer, which could decrease the catalytic activity, similar to the conclusion reached in the former report.[105] Furthermore, a positively charged PAMAM dendrimer along with negatively charged poly(styrene sulfonate) or poly(acrylic acid) were used to prepare a layer-by-layer (LBL) film as a nanoreactor for accommodating Ag NPs.[103] However, the diffusion barrier existing in the multilayer film is likely to be strong, especially the barrier generated by linear polyanions that might block the 4NP anion diffusion during the catalytic reduction of 4NP by $NaBH_4$ as a reducing agent. The schematic illustration of the composite LBL film containing the Ag nanocatalyst is given in Fig. 3.

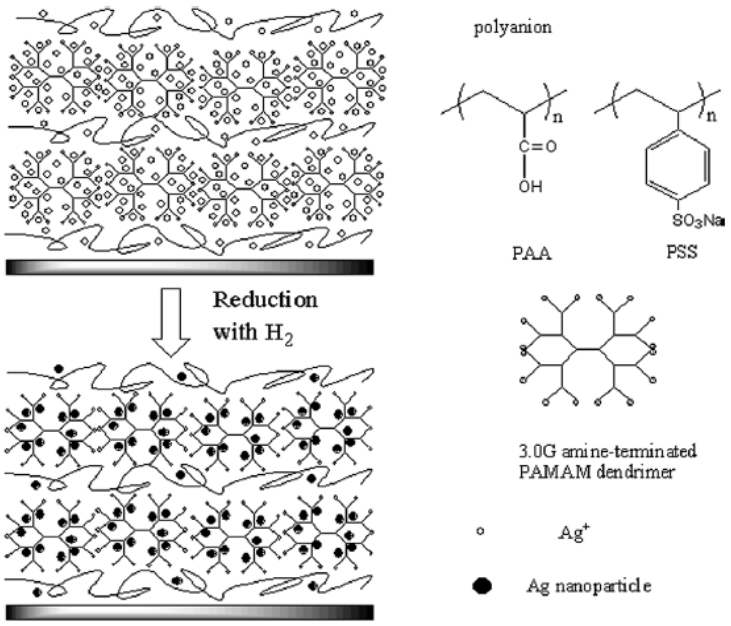

Fig. 3 Schematic presentation of preparation of the LBL multilayer film containing Ag nanocatalyst, together with the structural formulas of polyelectrolytes.[103]

A polyacrylonitrile (PAN) matrix was also used to immobilize Ag NPs through imbedding the Ag NPs inside the polymer matrix.[156] Such a PAN/Ag NPs composite is obviously unsuitable for catalytic applications due to the blocking effect of the polymer matrix. In this regard, Ag NPs were also reported to deposit on the surface of a PAN nanofiber in order to expose most of their clean surfaces.[157] Before deposition of the Ag NPs onto its surface, PAN nanofiber was pre-modified to incorporate binding sites. Hydroxylamine hydrochloride was used as the modifier via reaction with the –CN groups of PAN to yield many hydroxyl and amine groups that could immobilize silver ions through chelating effect. The Ag catalyst decorated on the modified PAN fiber was subsequently produced by reduction treatment. Furthermore, a poly-(3,4)ethylenedioxythiophene (PEDOT) matrix was reported as a support for Pd NPs.[64] To facilitate the subsequent catalytic reduction of 4NP, sodium polystyrenesulfonate (Na–

PSS) was used to help disperse the PEDOT-supported Pd NPs in an aqueous dispersion, However, a deleterious effect of the surfactant Na-PSS on the catalytic reaction should be paid attention since the surfactant was most likely to positon the Pd catalyst. A conducting polymer, namely polypyrrole (PPy), was also employed to stabilize Fe_3O_4 and Au NPs,[158] but these NPs were imbedded or wrapped by the polymer matrix, which indicates an enormous diffusion barrier to the catalysant, in this case MB dye, and hence deleteriously affects the catalytic properties.

Poly(allylamine hydrochloride)-modified poly(glycidyl methacrylate) composite sub-microspheres were also reported as a carrier system for an Au nanocatalyst.[84, 159] It was found that the epoxy groups and positive charges of the carrier system could benefit the catalytic reaction. Due to their electrophilicity, the epoxy groups could work as electron acceptor to attract electrons, likely leading to an electron-enriched region at the interface of Au NPs and sphere. Such a region could thereby serve as reservoirs for electrons and thus facilitate electron transfer to the reactant 4NP during the catalysis of the 4NP reduciton; meanwhile, the 4NP anions could be readily adsorbed onto positively charged sphere surfaces via electrostatic interactions. However, apart from the rigorous preparation conditions and multistep procedures limiting the large-scale applications, the stability and reusability of the composite sphere catalyst are not investigated. Moreover, the electrons trapped by epoxy groups might not be easily released, and the epoxy groups can also be reduced by the captured electrons during the catalytic reduction reaction.

PS quaternary ammonium resin beads were also reported to stabilize Au NPs for catalyzing the reduction of 4NP.[160] It was found that the smaller the size of Au NPs, the higher the rate of the catalytic reaction. However, the Au NPs immobilized on the resin

surfaces seems unstable since they can be easily eluted by cationic surfactants, indicative of a low durability of the composite catalyst. More information about organic polymer-supported and stabilized metal NPs is summarized in Table 3.

Table 3 Summary of the polymer-supported and stabilized metal NPs for catalysis of the reduction reactions.

Metal catalyst	Stabilizer or Carrier System	Reductant 1	Catalysant/Substrate	Reductant 2	Solvent	Reaction Condition	Ref.
Ag or Au	calcium alginate gel beads	UV light irradiation (365 nm wavelength)	4NP	$NaBH_4$	water	ambient temperature, atmospheric condition	154
Ag	barium alginate gel beads	solar light irradiation	4NP	$NaBH_4$	water	ambient temperature, atmospheric condition	151
Ag	polyacrylic acid–amidodiol hydrogel	amidodiol	MB, rhodamine 6G (R6G), crystal violet	$NaBH_4$	water	room temperature	58
Pd	spherical polyelectrolyte brushes, core-shell microgels	$NaBH_4$ under an atmosphere of nitrogen	4NP	$NaBH_4$	water	room temperature	98
Co, Ni, Cu	poly(methacrylic acid) microgels	$NaBH_4$	Eosin Y, methyl orange, 2-nitrophenol, 4NP, 4-nitroaniline	$NaBH_4$	water	30 ^{o}C, 40 ^{o}C, 50 ^{o}C, 60 ^{o}C.	152
Co, Ni, Cu, Fe	poly(4-vinylpyridine) cryogels modifed by 1,4-dibromobutane	$NaBH_4$	MB, 4NP	$NaBH_4$	water	room temperature	153
Au	polymer dendrimers	$NaBH_4$	4NP	$NaBH_4$	water	room temperature, stirring	105
Au	polymer dendrimers	laser irradiation	4NP	$NaBH_4$	water	room temperature, stirring	106
Ag, Pt, or Pd	polymer dendrimers with surface amino groups	$NaBH_4$	4NP	$NaBH_4$	water	15 °C	155
Pd	poly-(3,4)ethylenedioxythiophene, Na-PSS	3,4-ethylenedioxythiophene	4NP	$NaBH_4$	water	room temperature	64
Au	poly(allylamine hydrochloride)-modified poly(glycidyl methacrylate)	trisodium citrate, $NaBH_4$, LAA	4NP	$NaBH_4$	water	22 ^{o}C, stirring	84, 159
Ag	'nano-tree' type PEGMA brushes	$NaBH_4$	4NP	$NaBH_4$	water	room temperature	97
Au	trisodium citrate, polystyrene quaternary ammonium resin in chloride form	trisodium citrate	4NP	$NaBH_4$	water	25 °C	160
Au	1,4-bis(terpyridine-4 -yl)benzene	trisodium citrate, tannic acid	4NP	$NaBH_4$	water	room temperature	161
Ag	PAN	$NaBH_4$	MB	$NaBH_4$	water	nitrogen atmosphere, magnetic stirring	157

Ag	sulfonated PS spheres (as templates), PVP (stabilizing agent)	PVP	R6G dye	KBH_4	water	room temperature, stirring	162
Ag	multilayer LBL films	hydrogen atmosphere (2 atm, 85 ◦C)	4NP	$NaBH_4$	water	room temperature	103

2.4. Metal catalysts carried by inorganic materials

2.4.1. Inorganic materials without graphene materials involved

SiO_2 has been widely reported as the metal catalyst support. For example, A Sn^{2+}-activated SiO_2 nanotube (SNT) was explored as a support for Au NPs.[81] The Sn^{2+} species linked to the activated SNTs could *in situ* reduce the metal salt to metal NPs. A good catalytic activity of the resulting composite catalyst was observed for the 4NP reduction. However, the synthesis is complex with multistep procedures, which may not be appropriate for economically feasible industrial production.[121] In addition, a recycling experiment is not considered in the work. A porous SiO_2 nanofiber was also explored to support a Ag nanocatalyst for the reduction of MB dye through a multistep synthesis process.[163] Apart from the unconsidered durability measurement of the composite catalyst, the tedious preparation process, along with the use of the undesirable volatile organic solvent and high-temperature processing, can cause a high production cost and an environmental problem, especially for large-scale applications. A mesoporous SiO_2 (SBA-15) was also used as a support to fabricate SiO_2/Cu NPs composite catalyst for the catalytic reduction of different kinds of aromatic compounds including 4NP, MB, RhB, Methyl Orange, and Congo Red.[1] It was observed that some formed Cu NPs were embedded in the pore channels of SBA-15, while some others were deposited on the SBA-15 surfaces. Most of the pores and nanochannels of SBA-15 remained intact after the loading of the Cu NPs, suggesting that this work did not achieve effective immobilization of Cu NPs within the pores and nanochannels of SBA-15. The Cu NPs

deposited on the SBA-15 surfaces, without a satisfactory confinement effect of the pores and nanochannels, are likely to leak out during the catalysis. Hollow SiO_2 particles were also used to stabilize a Ag nanocatalyst, but the formed Ag nanocatalyst completely located inside the hollow SiO_2 spheres, leading to a low efficiency in the catalytic reduction of MB dye because diffusion of the reactants in and out of the SiO_2 nanocontainers had to occur.[145]

In addition to SiO_2, Fe_3O_4 is another popular material for fabrication of metal-based composite catalysts mainly because of its magnetic properties that can render the resulting composite catalyst easily recyclable using an external magnetic field. For instance, as a movable core, a Fe_xO_y (a mixture of Fe_3O_4 and Fe_2O_3) was incorporated into a mesoporous SiO_2 ($mSiO_2$) shell whose inner surface was anchored with Pd NPs.[67] It was found that the composite catalyst showed a good durability because the Pd NPs were encapsulated by the $mSiO_2$ shell and thus well protected from aggregation and leaching. However, preparation of such a composite catalyst was quite complicated. The schematic presentation of the preparation process is also given in Fig. 4. Such a multistep synthesis process makes it laborious, time consuming and costly, thus limiting the practical applications. Concerning the catalytic property, the presence of the $mSiO_2$ covering layer can bring about a strong diffusion barrier to impede the 4NP molecules from contacting with the Pd NPs during the catalytic reaction, which can largely decrease the catalytic efficiency. Using a similar method to that presented in the aforementioned report,[81] a Fe_3O_4@SiO_2–Au magnetic composite catalyst was also fabricated,[164] i.e., Sn^{2+} species, as linked to the Fe_3O_4@SiO_2 by inorganic grafting, were used to *in situ* reduce Au^{3+} to Au NPs.

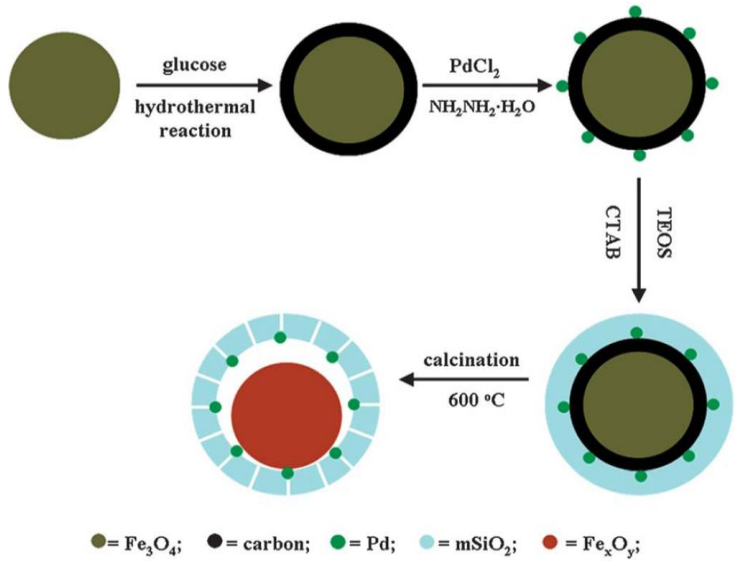

Fig. 4 Schematic presentation of the preparation process of FexOy/Pd@mSiO$_2$ composite. Reproduced from Ref. 67 with permission from The Royal Society of Chemistry.

As an allotrope of graphene, CNT has been well used as a support for metal catalysts.[92, 165-167] For instance, a Ag catalyst was immobilized on multiwalled CNTs with COOH groups as the anchoring sites.[92] The CNTs with COOH groups were also explored to support and stabilize Fe_3O_4 and Au NPs by virtue of a nucleation effect of the COOH groups.[167] However, the oxygen groups might be unstable during the catalytic reduction reaction with $NaBH_4$ as a reducing agent. If the COOH groups are reduced, the aggregation or leaching of Ag or Au catalyst will be likely to take place.

Many other kinds of inorganic materials have also been explored as supports for metal catalysts. For example, a nanocrystalline MgO (NAP-MgO) was used to stabilize a palladium(0) catalyst.[168] It was found that the reaction between Na_2PdCl_4 and NAP-MgO played an important role in the synthesis process. While the Na^+ ions could interact with the O^{x-} sites/anionic vacancies, $PdCl_4^{2-}$ ions were presumed to interplay with the Mg^{2+} sites/cationic vacancies being present at corners or edges of NAP-MgO. The as-

synthesized composite catalyst was used for the selective reduction of a variety of nitro compounds. In addition, Al_2O_3 was reported as a support for a Ni catalyst.[169] It was found that the catalytic activity of the composite catalyst was strongly dependent on the size of the Al_2O_3 particles used. The smaller the size of the Al_2O_3 particles, the lower the catalytic activity. A silicon nanowire array was also reported as a support for a Cu nanocatalyst via galvanic displacement reaction, but highly corrosive chemical agents were involved such as hydrofluoric acid and piranha solution.[133]

More information about the study on inorganic material-supported metal catalysts (except for using inorganic graphene materials as the support) for the reduction of dye and nitro compounds is summarized in Table 4.

Table 4 Summary of the catalytic reduction reactions over the inorganic material-supported metal catalysts (except for using graphene-based material as support).

Metal catalyst	Stabilizer or Carrier System	Reductant 1	Catalysant/Substrate	Reductant 2	Solvent	Reaction Condition	Ref.
Pd	nanocrystalline MgO, SiO_2, C, or MgLaO	hydrazine hydrate	aromatic and aliphatic nitro compounds	molecular hydrogen	THF, DMF, toluene, methanol, iPA	ambient temperature, atmospheric pressure, stirring	168
Pd	mesoporous SiO_2	hydrazine hydrate	4NP	$NaBH_4$	water	room temperature, stirring	67
Ni	nonporous Al_2O_3	hydrazine hydrate	4NP	molecular hydrogen	ethanol	magnetic stirring, 102 °C, 1.65 MPa	169
Cu	mesoporous silica SBA-15	$NaBH_4$	4NP, MB, RhB, Methyl Orange, Congo Red,	$NaBH_4$	water	room temperature	1
Ag	porous silica nanofibers	calcination of silica-PMCM hybrid fibers containing $AgNO_3$ at high temperatures	MB	$NaBH_4$	water	room temperature, under nitrogen, stirring	163
Cu	silicon nanowire arrays	galvanic displacement reaction	MB, RhB, 4NP	$NaBH_4$	water	room temperature, stirring	133
Au	Fe_3O_4@SiO_2–Sn^{2+}	Sn^{2+} moiety of Fe_3O_4@SiO_2–Sn^{2+}, sodium formate	4NP	$NaBH_4$	water	room temperature	164

Ag	Fe_3O_4@SiO_2	*n*-butylamine	RhB, Eosin Y	$NaBH_4$	water, water mixed with surfactant or Na_2SO_4	room temperature	96
Au	Fe_3O_4 NPs decorated CNTs	ethylene glycol	4NP	$NaBH_4$	water	room temperature	167
Ag	–COOH functionalized MCNTs by treating with HNO_3	electrochemical process	R6G, orange G	$NaBH_4$	water	room temperature, shaking	92
Au	electrospun SNTs [a]	Sn^{2+} linked to the surfaces of SNTs	4NP	$NaBH_4$	water	room temperature, stirring	81
commercially available Au/TiO_2, Au/Al_2O_3, and Au/ZnO (~1 wt.% in Au)			various nitro compounds	hydrazine	ethanol	at 60 °C, under an inert atmosphere	170
Pt/C, Ni/C, Pd/C, Ru/C, Rh/C, Pt/Al_2O_3, Pt/SiO_2, Pt/HY (commercial products)			4NP	molecular hydrogen	water, methanol, ethanol, nPA, nBA	35-80 °C, stirring	171

Note:

[a] Silica nanotubes

2.4.2. Unmodified graphene materials as supports for metal catalysts

Many attempts have been made to employ graphene materials, especially GO-based ones, as supports for metal catalysts. As compared to other popular carbon materials, viz. CNTs, the lower cost and accessibility of both the bottom and top surfaces make graphene materials superior as the catalyst support.[172] GO can also be directly used to bind a large number of metal NPs by virtue of its large specific surface area and many anchoring sites on its surfaces such as oxygen functionalities and structural defects. Nevertheless, GO is susceptible to chemical and thermal impact attributable to its labile oxygen functionalities, which thus causes variability of the pure GO support and hence concomitant instability of the metal nanocatalyst deposited on its surfaces. For example, during the catalytic reduction reaction, some oxygen groups can be chemically reduced, which likely makes the metal NPs deposited on these sites unstable. This might

eventually lead to the leaching and congregation problems. In this subsection, we will present a review of some typical work devoted to studying the unmodified graphene material-supported metal catalysts for the aromatic pollutant reduction.

A hybrid of RGO sheets and Au NPs was fabricated in an aqueous phase using GO and $HAuCl_4$ as the starting materials under UV light irradiation.[173] The intense UV light irradiation could allow the formation of hot and reactive spots that localized at the GO sheets and their close vicinity in the aqueous phase. Such hot and reactive spots were proposed as the origin for conversion of $AuCl_4^-$ to Au NPs, as well as for reduction of GO to RGO. In addition, a RGO-supported Pt NPs prepared by an ethylene glycol (EGly) reduction approach was explored for the catalytic hydrogenation of nitroarenes.[172] EGly exhibited more advantages than commonly used hydrazine hydrate in fabrication of mono-dispersed Pt NPs of small size deposited on the RGO surfaces. It was also found the catalytic activity of the EGly-RGO-supported Pt was superior to other carbon allotropes (including CNT and active carbon)-supported Pt catalysts, which could be attributed to the better-dispersed Pt clusters on the RGO sheets and to the better dispersion state of the hybrid catalyst in the catalytic reaction solution. A self-assembled RGO hydrogel was also reported as a carrier system for Au NPs.[47] A one-pot hydrothermal reaction was adopted to produce the graphene hydrogel-immobilized Au nanocatalyst for the reduction of 4NP and MB. As the starting material, GO could be converted effectively to a RGO after the hydrothermal reaction, along with significantly decreased oxygen groups, which thus suggests that the complexation and binding sites might not be sufficient for stabilizing a large number of Au NPs on the RGO surfaces if without an additional modification or functionalization treatment. Due to the violent

catalytic reaction in the presence of $NaBH_4$, the self-assembled graphene hydrogel may also not be so strong as to resist the impact from the catalytic reaction, indicating the high probability of disintegrating the physically assembled hydrogel without chemical cross-links. A reusability test is also not considered in the study. Furthermore, it was reported that noble metal ions and GO sheets could be reduced simultaneously by a combined effect of active metal Zn (or Mg) and hydrochloric acid (or sulfuric acid), leading to noble metal-RGO hybrid catalysts.[174, 175] During the synthesis, the active metal Zn or Mg could convert the noble metal ions to the corresponding metal NPs via galvanic replacement reaction, while the H_2 gas formed by the reaction between the active metal and acid medium was capable of reducing GO to RGO. However, a shortage of anchoring sites on RGO might make the hybrid catalyst un-reusable as a consequence of the instability of the noble metal NPs deposited on RGO. A durability test is also not considered in the study.

A composite structure composed of Ag, GO and Bi_2O_3 was explored as a catalyst for the reduction of 4NP by $NaBH_4$.[176] It was found that both the GO and Bi_2O_3 could be *in situ* reduced to RGO and metallic Bi respectively by $NaBH_4$ during the catalysis, which thus suggested that the main role in the catalytic reduction was played by both Ag and Bi. This result also offers us an indication that some metal oxides can be reduced to their zero-valent metallic counterparts under the commonly used catalytic reaction condition with $NaBH_4$ as a reducing agent, so the catalytic origin should be the zero-valent metal rather than the metal oxides. A laser-converted graphene was also reported to support an Au nanocatalyst for the reduction of different kinds of dyes including MB, RhB, Sulforhodamine 101 hydrate, and Fluorescein.[177] However, the Au NPs might not be able

to well stabilize on such a graphene since the graphene moiety appears to only serve as a holder for the Au NPs ablated during laser ablation of a gold strip, revealing weak interactions between the graphene and Au NPs. Furthermore, a commercial graphene material was employed to carry a Ag nanocatalyst for the reduction of MB dye.[52] Such a graphene/Ag nanocomposite was prepared by a solid-state thermal decomposition approach. However, the hybrid catalyst appears to have a poor reusability since a significant loss of catalytic activity can be observed after 3 runs of repeated usage, as verified in Fig. 5(a). Such a loss can be attributed to the aggregation of Ag NPs, as evidenced by SEM images of the catalyst before and after used for the catalytic reaction (shown in Fig. 5(b) and 5(c) respectively). The following aspects might cause the instability of the Ag nanocatalyst: (i) the lack of binding sites on the surfaces of commercial graphene sheets such as oxygen groups and structural defects, (ii) without additional incorporation of binding sites onto the commercial graphene sheets by means of modification and functionalization, and (iii) the violent catalytic reaction in the presence of $NaBH_4$ as a reducing agent that likely pushes the Ag NPs to aggregate. Therefore, a modification or functionalization treatment of pure graphene is usually necessary for incorporating sufficient binding sites before decoration of metal catalyst on the graphene surfaces, in order to produce a stable and durable graphene-based composite catalyst for the catalytic reduction reactions.

More information about the work devoted to using unmodified graphene materials as supports for metal catalysts is summarized in Table 5.

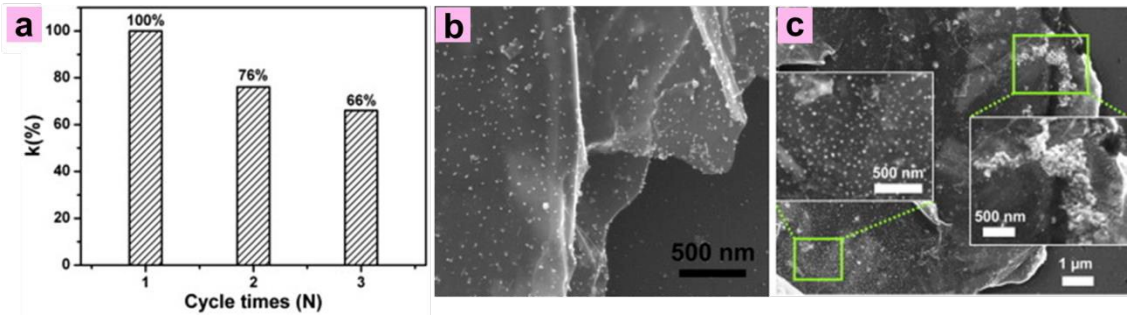

Fig. 5 (a) Recycling experiments of the Ag/graphene catalysts in reduction of MB. (b, c) SEM images of Ag/graphene nanocomposite before (b) and after (c) used for the catalytic reaction.[52]

Table 5 Summary of the unmodified graphene-supported metal nanocatalyst for aromatic pollutant reductions.

Metal catalyst	Stabilizer or Carrier System	Reductant 1	Catalysant/Substrate	Reductant 2	Solvent	Reaction Condition	Ref.
Au	laser converted graphene	laser ablation	MB, RhB, Sulforhodamine 101 hydrate, Fluorescein	$NaBH_4$	water	room temperature	177
Au	self-assembled graphene hydrogel	triethylenetetramine, hydrothermal (180 ^oC)	4NP, MB	$NaBH_4$	water	room temperature	47
Ag, Bi	GO, α-Bi_2O_3, RGO (*in situ* formed during the catalytic reaction)	heating the undoped composites in $AgNO_3$ solution at 80 °C (for Ag), *in situ* reduction by $NaBH_4$ during the catalysis (for Bi)	4NP	$NaBH_4$	water	under ice-cold conditions	176
Au	UV-reduced GO (RGO)	UV light irradiation (generated by a 50W short arc mercury bulb, irradiated in the 280–450 nm wavelength range)	p-nitroaniline	$NaBH_4$	water	room temperature	173
Pt or Pd	RGO	Mg ribbon and HCl solution	4NP	$NaBH_4$	water	room temperature, stirring	175
Au, Pt, Pd and Ag	RGO	metallic Zn power and H_2SO_4 solution	4NP	$NaBH_4$	water	room temperature, sonication, shaking	174
Pt	RGO	ethylene glycol	nitroarenes	molecular hydrogen	ethanol	0-40 ^oC, magnetic stirring	172
Pd, Pt, Au, Ag	RGO	ethylene glycol, $NaBH_4$	potassium hexacyanoferrate(III)	$NaBH_4$	NaOH aqueous solution	saturated with N_2, room temperature	178
Au	low-defect GSs	electrochemical exfoliation of graphite, trisodium citrate dihydrate, microwave-assisted	ethyl benzoate	$NaBH_4$	water	room temperature, continuous stirring	179
Ag	commercial GSs	thermal treatment at 250 ^oC under vacuum	MB	$NaBH_4$	Na_2CO_3/$NaHCO_3$ buffer solution	pH: 9.5, room temperature	52

2.5. Modified inorganic material-stabilized metal catalysts and inorganic material-supported surface-modified/protected metal catalysts

To produce a stable metal catalyst deposited on the inorganic material for the catalytic reduction reactions, some typical approaches are summarized as follows: (i) the inorganic support material is pre-modified or functionalized (in most cases by an organic material) to incorporate effective anchoring sites onto its surfaces followed by binding with the metal NPs; (ii) the metal catalyst is pre-modified to introduce interactive sites onto its surfaces for subsequently attaching to the inorganic support via π-π stacking interactions, van der Waals forces, electrostatic interactions, or other molecular interactions; (iii) the metal NPs deposited on an inorganic support were further protected by a surfactant, ligand, and/or penetrable porous organic or inorganic layer to protect them from aggregation on the inorganic support; (iv) combination of two or more approaches as listed above. Some reported methods can well stabilize the metal NPs and also keep their surfaces accessible to the reactants during the catalysis, thus allowing the catalytic activity to be not heavily affected; e.g., covering a penetrable porous layer around a metal catalyst surface, with little barrier to the diffusion of the reactant molecules. On the other hand, some others establish the stability of metal NPs on the basis of lowering the catalytic activity; e.g., passivation or blocking of metal catalyst surfaces to fabricate a durable catalyst.

2.5.1. Non-graphene materials involved

SiO_2 has been widely employed as an inorganic core to fabricate metal-based

multicomponent composite catalysts. For example, before used as a support for Ag NPs, SiO_2 spheres were functionalized with 3-aminopropyltrimethoxysilane.[45] The Ag NPs could be stabilized on the functionalized silica spheres due to the aminophilic nature of the Ag NPs and to the electrostatic interactions between the Ag NPs and amidogen of the functionalized SiO_2. The resulting composite catalyst was employed to catalyze the reduction of three differently charged dyes, namely MB, eosin and rose Bengal, using $NaBH_4$ as a reducing agent. As a result of the cathodic polarization by BH_4^- ions, the composite catalyst had a stronger affinity to the positively charged dye than to the negatively charged one due to the electrostatic interactions. A polyethyleneimine was also reported to modify SiO_2 spheres in order to introduce binding sites for the subsequent stabilization of Ag NPs.[180] Surfactant CTAB was also used as a stabilizer during the Ag seed-mediated growth process, but it might poison the catalyst and lower the catalytic performance, as demonstrated in the Ref.[45] Additionally, SiO_2 spheres and complexant PVP were explored to support and stabilize Ag NPs through first adsorbing $[Ag(NH_3)_2]^+$ ions onto the SiO_2 spheres based on electrostatic interactions between the $[Ag(NH_3)_2]^+$ and silanol groups of the SiO_2, and then reducing the adsorbed $[Ag(NH_3)_2]^+$ and protecting the formed Ag NPs with PVP as both a reducing agent and complexant.[51] However, the stabilizer PVP introduced could strongly adsorb on the surfaces of Ag NPs, which is likely to cause the degradation of the catalytic performance of the composite catalyst, as described in the Refs.[52, 87] A composite nanosphere consisting of a SiO_2 core, poly(dopamine acrylamide-co-methacrylic acid-co-ethylene glycol), and Ag NPs was also reported as a catalyst for the reduction of 4NP and R6G dye.[181] However, the preparation process is complex, with long synthetic steps, which might inhibit the large-

scale application of the composite nanospheres. In addition, recycling of the composite nanospheres seems difficult, as high-speed centrifugation is required, making the process time-consuming and labor-intensive.

In addition to SiO_2, Fe_3O_4 has also drawn significant attention as a basic inorganic core to fabricate composite catalysts. For instance, a chitosan-coated Fe_3O_4 was reported as a magnetic nanocarrier to immobilize Au NPs.[182] The chitosan layer coated on Fe_3O_4 NPs provided a driving force for the formation and stabilization of Au NPs. It was found that the catalytic reduction of 4NP over the prepared composite catalyst was diffusion-determined, similar to that observed for the reduction of 4NP over the dendrimer-encapsulated metal catalyst.[155] A chitosan layer was also reported to attach to a modified Fe_3O_4 core as a support for Au NPs for the catalytic reduction of different kinds of dye compounds and 4NP.[3] However, the multistage procedures and many hazardous chemicals involved such as volatile organic solvents might make the preparation process undesirable for large-scale applications.

Apart from using chitosan as a modifier, L-Lysine was also employed to modify a Fe_3O_4 core with surface OH groups for introducing NH_2 groups onto the Fe_3O_4 core, followed by binding of Cu^{2+} ions to the modified Fe_3O_4 core through Cu^{2+}-NH_2 complexation.[56] The composite catalyst was produced after reduction of Cu^{2+} to Cu NPs, and then applied to the catalytic reduction of different kinds of dyes and 4NP. A PANI polymer was also reported to modify a Fe_3O_4 core by an *in situ* surface polymerization method with the assistance of SDS.[7] The resulting core–shell Fe_3O_4@PANI was then used to support and stabilize Au NPs through electrostatic interactions. Furthermore, 1,6-hexadiamine was reported to functionalize a Fe_3O_4 core before deposition of a metal-

based catalyst onto the core.[183] The 1,6-hexadiamine could work as both a stabilizer and precursor for *in situ* incorporation of the amino groups into the Fe_3O_4 clusters. A PVP-stabilized Ag@Pd nanocatalyst was separately prepared and then assembled onto the functionalized Fe_3O_4 NPs via the attractive interactions between metallic colloids and amino groups of the functionalized Fe_3O_4 NPs. However, because the Ag composition is completely encapsulated by the Pd shell, the Ag core cannot be accessed in the catalytic reaction, indicating the waste of noble metal Ag. If the Ag core can be replaced by other cheaper materials such as non-noble metal, the production cost can be reduced and the catalytic performance might not be affected. Dumbbell- and flower-like Au-Fe_3O_4 composite catalysts were also prepared through thermal decomposition of the iron-oleate complex in the presence of Au NPs of different sizes as the seeds.[184] However, many kinds of organic stabilizers, reducing agents and solvents were used in the preparation process, which can make the synthesis expensive and hazardous and thus limit the large-scale applications.

In addition to a Fe_3O_4 core, an additional inorganic SiO_2 interlayer was also incorporated before further organic modification with a polyamidoamine dendrimer and then immobilization of Ag NPs in the dendrimer.[185] However, the structural features of the composite catalyst are not clearly exhibited by SEM or TEM, with only aggregated NPs discernable. This might be caused by the interactions of metal NPs with polydentate nitrogen-containing ligands that most often result in quick aggregation because of rapidly bridging and bonding adjacent NPs together.[161]

Besides functionalization of a Fe_3O_4 core for well stabilizing a metal nanocatalyst, a metal–organic framework (MIL-100(Fe)) layer was further used to protect the metal

nanocatalyst being deposited on the functionalized Fe_3O_4 core.[186] Specifically, after fabrication and functionalization of the Fe_3O_4 core with L-cysteine, Au NPs were stabilized on the functionalized core, followed by surface modification of the Au NPs with mercaptoacetic acid. Finally, the MIL-100(Fe) layer was covered onto the modified Au NPs@Fe_3O_4 using a LBL assembly method. It was found that the catalytic performance of the as-prepared Fe_3O_4@Au@MIL-100(Fe) composite was highly dependent on the thickness of the framework layer which could bring about a diffusion barrier to the reactants during the catalysis. It is also possible that the presence of the mercaptoacetic acid on Au surfaces might poison the Au nanocatalyst.[187] Furthermore, the long synthetic steps are most likely to limit the large-scale applications.

Interestingly, rather than being deposited on an inorganic support, Ag NPs were encapsulated in the aggregates of Fe_3O_4 particles to form a so-called core–shell Ag/Fe_3O_4 structure as a catalyst for the reduction of Rhodamine B (RhB) dye,[53] as displayed in Fig. 6. Since the Ag core served as the catalytic center for electron relay, the Fe_3O_4 shell (strongly attached to the Ag core) might impede the diffusion of dye molecules to the Ag catalyst surfaces, as shown in Fig. 6(b). On the other hand, most of the Fe_3O_4 NPs loosely lying around the Ag cores can also be observed from the TEM image presented in Fig. 6(a), which makes the catalytic reaction work. However, such loose aggregates of Fe_3O_4 NPs are likely to be unstable by considering that they might be disentangled under the impact from violent catalytic reaction under stirring/agitation, which thereby indicates the possible instability of the core–shell Ag/Fe_3O_4 hybrid structure. PVP was also used during the synthesis, which might poison the hybrid catalyst and degrade its activity since it has been reported that the presence of PVP in the catalytic solution can block the

catalytic reduction reaction.[87, 94]

More information about the functionalized/modified inorganic material-stabilized metal catalyst and inorganic material-supported surface-modified/protected metal catalyst (without graphene materials involved) is summarized in Table 6.

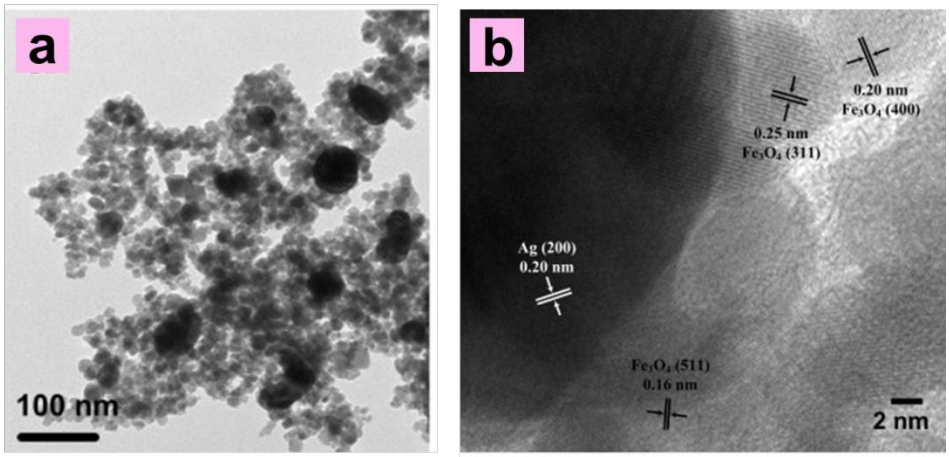

Fig. 6 a,b) Low-resolution (a) and lattice-resolved high-resolution (b) TEM images of a Ag/Fe_3O_4 nanocomposite.[53]

Table 6 Summary of the modified inorganic material-stabilized metal catalysts and inorganic material-supported surface-modified/protected metal catalysts (without graphene materials involved).

Metal	Stabilizer or Carrier System	Reductant 1	Catalysant/Substrate	Reductant 2	Solvent	Reaction Condition	Ref.
Ag	3-aminopropyltrimethoxysilane-functionalized silica spheres	$NaBH_4$	MB, EO, and RB	$NaBH_4$	water, water mixed with surfactant or electrolyte	room temperature, stirring	45
Au	non-functionalized SiO_2, aminopropyl-functionalized SiO_2, mercaptopropyl-functionalized SiO_2	$NaBH_4$	MB, thionine, proflavine	$NaBH_4$	water, water mixed with surfactant	room temperature	44
Ag	copolymer, SiO_2	catecholamine moieties of the copolymer	4NP, R6G	$NaBH_4$	water	room temperature	181
Au	chitosan-coated Fe_3O_4	$NaBH_4$	4NP	$NaBH_4$	water	room temperature, constant stirring	182
Ag@Pd core–shell NPs	PVP, hexadiamine, amino-functionalized Fe_3O_4	ethylene glycol	4NP	$NaBH_4$	water	room temperature	183
Au	oleylamine, oleic acid, sodium citrate, Fe_3O_4	*tert*-butylamine borane complex, oleylamine	4NP, 2,4-dinitrophenol	$NaBH_4$	water	room temperature	184

Au	PPy/Fe_3O_4 capsule shell	sodium citrate	MB	$NaBH_4$	water	room temperature	158
Au	Na_3citrate, Fe_3O_4@PANI composites	$NaBH_4$	Congo red	$NaBH_4$	water, water mixed with electrolyte or surfactant	25 ^oC, under continuous stirring	7
Cu	Fe_3O_4, L-Lysine	$NaBH_4$	MB, methyl red, methyl orange, 4NP	$NaBH_4$	water	room temperature	56
Au	alkyl-functionalized Fe_3O_4, chitosan	trisodium citrate, glucose	4NP, MB, Congo red, RhB, R6G, acid orange, methyl orange	$NaBH_4$	water	room temperature, stirring	3
Ag	Fe_3O_4, 3-aminopropyl triethoxysilane, polyamidoamine dendrimer, PVP	PVP, refluxed by stirring at 70 ^oC	4NP	$NaBH_4$	water	room temperature	185
Ag (core)	Fe_3O_4 (shell), PVP	PVP, hydrothermal treatment	RhB	$NaBH_4$	water	room temperature, stirring	53
Ag	SiO_2 sphere, polyethyleneimine, CTAB	$NaBH_4$ (for seed), ascorbic acid (for growth)	4NP	$NaBH_4$	water	room temperature	180
Ag (core)	CTAB, SiO_2 (frame)	ascorbic acid	4NP	$NaBH_4$	water	different temperatures (20–90 ^oC)	188
Ag	SiO_2, PVP	PVP	RhB, BR K-2BP	KBH_4	water	room temperature, stirring	51
Ag	boron nitride nanosheets, PVP	glucose	4NP	$NaBH_4$	water	room temperature	94
Au	mercaptoacetic acid, metal-organic framework (MIL-100(Fe))	formaldehyde	4NP	$NaBH_4$	water	room temperature	189
Au	L-cysteine, Fe_3O_4 mercaptoacetic acid, organic framework (MIL-100(Fe))	L-ascorbic acid	4NP	$NaBH_4$	water	room temperature	186
Au	commercial SiO_2 functionalized with polyethylenimine	Polyethylenimine moiety	4NP	$NaBH_4$	water	25 °C	104
Ag	commercial SiO_2 functionalized with polyethylenimine	Polyethylenimine moiety	MB, Sunset Yellow, Azorubine	$NaBH_4$	water	25 °C	190
Au	alkyne-functionalized nano-SiO_2	alkynyl carbamate moieties	4NP	$NaBH_4$	water	25 °C	191

2.5.2. Graphene-based materials involved

GO sheets have been commonly used as a basic support for further surface modification and then binding with metal catalysts. For example, ethanediamine-modified GO sheets were used as a support for an Au catalyst.[192] A phenolic hydroxyl-rich tannic acid (TA) was also explored as both reducing and immobilizing agents for producing and stabilizing an Au catalyst on GO sheets,[82] but the structural details of the graphene component of the composite catalyst are not provided even though it is important to know whether the TA can reduce GO to a RGO; e.g., the improved π system of the RGO can play an important role in the catalytic reaction as a result of its electron

shuttling properties and adsorption capacity of 4NP molecules via π-π interactions.

Rather than use of single GO as a basic inorganic support, a composite of Fe_3O_4 and GO was explored to support Au NPs.[193] The Fe_3O_4 NPs were first deposited on the GO surfaces in 1-methyl-2-pyrrolidone solvent through complexation interactions between Fe_3O_4 and COOH groups of GO. The deposited Fe_3O_4 NPs were then surface-modified with 3-aminopropyltriethoxysilane in an ethanol/water solvent. Au seeds was prepared separately and then combined with the NH_2 groups of the modified Fe_3O_4 NPs, followed by growth of the Au seeds to produce the composite catalyst. It was found that Au shells were formed on some Fe_3O_4 NPs, along with the Au NPs attached to the GO-based composite support. However, regardless of the complex preparation process with the use of undesirable organic solvents making it less likely for large-scale applications, GO might be unstable under the catalytic reduction condition with $NaBH_4$ as a reducing agent because the reduction of COOH groups could bring about an overall instability of the composite catalyst; e.g., causing aggregation of Fe_3O_4 and Au NPs.

Our group has recently reported multicomponent composite catalysts consisting of a chemically or thermally functionalized graphene (derived from GO), polymer structure and metal catalyst,[33, 49] as shown in Fig. 7. These composite catalysts could be conveniently synthesized through water-based routes. A mussel-inspired modification and functionalization of GO was applied to the production of the chemically functionalized graphene (also a kind of RGO) that was subsequently employed to nucleate and stabilize Cu NPs, resulting in a well-structured quasi-2D composite catalyst (Fig. 7(a)).[33] As a control, a lack of Pdop coating could lead to aggregation of Cu NPs into Cu particles of large size being far beyond nano-sized range. Due to the strong van

der Waals and π-π staking interactions between pure RGO layers [109], the aggregation of RGO sheets could also take place (top part of Fig. 7(a)). The mechanism of the efficient catalytic reduction of different dye compounds over the Cu nanocatalyst stabilized by Pdop-modified GSs was also described (bottom part of Fig. 7(a)). We also fabricated a multicomponent composite catalyst with a monolithic structure consisting of a polyacrylamide (PAM) hydrogel network, low-temperature thermally functionalized graphene and Ag nanocatalyst (Fig. 7(b)).[49] The synergistic effect of the ternary components was well demonstrated in this study. The use of PAM network could play several roles which include enabling the PAM-based composite catalyst to be easily handled, providing the composite catalyst with double crosslinking network to highly stabilize the Ag catalyst, and rendering the composite catalyst adsorptive due to its porosity. Finally, the mechanistic insight into the highly efficient reduction reactions catalyzed by the composite catalyst was described, as also shown in the bottom part of Fig. 7(b).

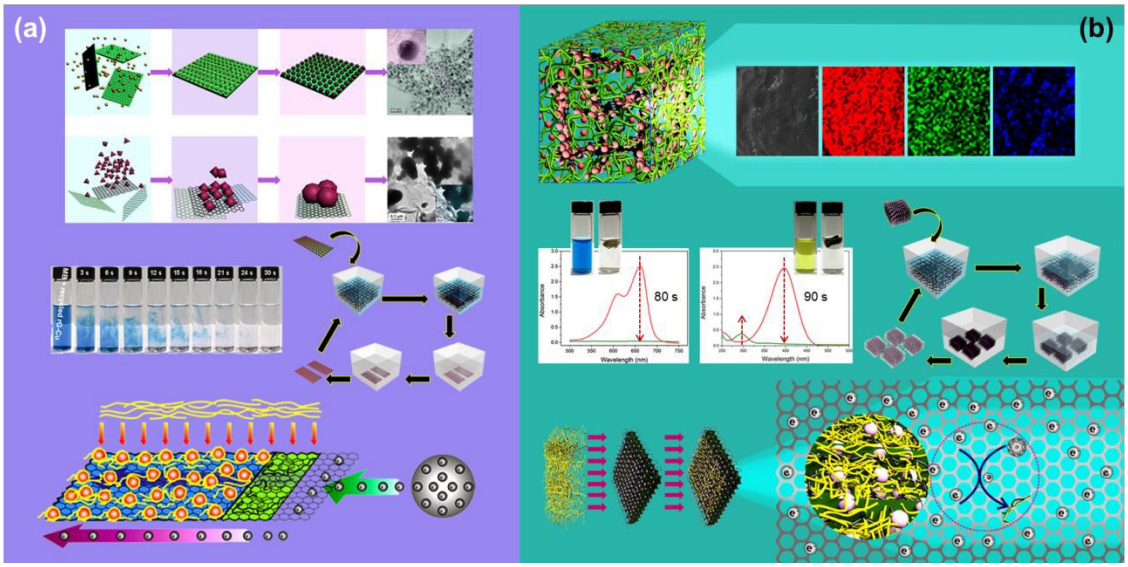

Fig. 7 Our work devoted to stabilization of metal catalysts using organic polymer structure combined with inorganic material, in this case a chemically or thermally

functionalized graphene.[33, 49] The main content relating to a quasi-2D composite catalyst being composed of a Pdop layer, chemically functionalized graphene and Cu catalyst is given in **Fig.** 7(a).[33] The main content associated with a 3D monolithic composite catalyst being consisting of a PAM network, functionalized graphene and Ag catalyst are presented in **Fig.** 7(b). Reproduced from Ref. 49 with permission from The Royal Society of Chemistry.

Instead of pre-modification of a graphene support to introduce binding sites, an Au nanocatalyst was pre-modified with 4-dimethylaminopyridine and then coupled with negatively charged GO via electrostatic self-assembly.[194] The π-π stacking interactions between the residual π-conjugated domains on GO sheets and the aromatic moiety of the stabilizer coated on the Au nanocatalyst could also assist the stabilization of the Au catalyst. However, the negatively charged COO^- of the GO support is likely to be chemically reduced during the catalytic reaction with $NaBH_4$ as a reducing agent, indicating that the initial electrostatic interactions might be weakened and hence resulting in the instability of the Au nanocatalyst deposited on the GO surfaces. Furthermore, an Au nanocatalyst was pre-modified with 2-mercaptopyridine and then combined with GO and RGO sheets to produce the hybrid catalysts for the *o*-nitroaniline reduction.[195] It was found that directly mixing the GO sheets and unmodified Au NPs could not lead to the Au NPs being effectively anchored on the GO sheets, thereby indicating that the 2-mercaptopyridine played an important role in stabilizing the Au NPs on the GO sheets. Nevertheless, some aggregates of the modified Au NPs are still observed on the GO surfaces, which might reveal that the binding sites on the GO surfaces are insufficient or the interactions between the anchoring sites and the modified Au NPs are not sufficiently high. This might cause instability of the modified Au NPs on the GO sheets. As a result, the durability of the hybrid catalyst is likely to be low even though a durability

measurement is not considered in the study. The presence of the 2-mercaptopyridine might also poison the Au catalyst and lower its catalytic performance.

In addition to use of GO and RGO as basic supports for metal catalysts, other kinds of graphene-based materials have also been explored. For instance, a high-quality few-layer graphene prepared by an electrochemical exfoliation approach was reported as basic support for an Au catalyst.[196] Before deposition of the Au catalyst on their surfaces, the high-quality graphene sheets were functionalized with bromoacetonitrile as a nitrogen source to form an N-functionalized graphene (N-GSs). However, the mechanisms of stabilization of the Au NPs on the N-GSs is not explained in the report, with focus only on the synthesis and analysis of the N-GSs. A durability test is also not considered, and the hybrid catalyst might not be reusable due to a shortage of binding sites as a consequence of a low extent of the N functionalization of the high-quality few-layer GSs. This also corroborates that GO and GO-derived graphene materials are more suitable as the support for the metal catalyst as compared to high-quality graphene materials.

Rather than to support the metal catalyst on its surfaces, a nitrogen-doped graphene was reported to wrap a FeCo nanocrystal.[79] A nitrogen–contained metal–organic framework $Fe_3[Co(CN)_6]_2$ spheres were first prepared and then annealed under a nitrogen atmosphere to obtain the FeCo nanocrystals encapsulated in the nitrogen-doped graphene layers. The obtained composite catalyst was then applied to the 4NP reduction. The overall preparation process is also presented in Fig. 8. However, the mechanism of the interactions between FeCo NPs and N-doped graphene is not clarified in the report. In addition, the encapsulation of the FeCo nanocatalyst in the N-doped graphene shell might seriously impede the diffusion of the 4NP molecules into the FeCo core during the

catalytic reaction. Moreover, the kinetics and mechanism for the catalytic reaction might be more complicated than envisioned by considering that the catalytic activity can also originate from the N-doped graphene shell, since an N-doped graphene has been demonstrated to effectively catalyze the reduction of 4NP.[197] More information about the relevant work categorized in this subsection is summarized in Table 7.

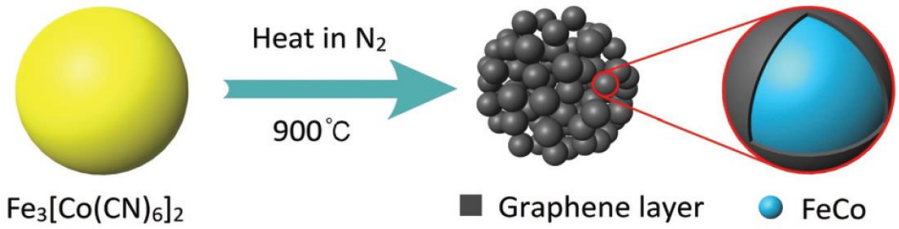

Fig. 8 Illustration of the synthesis of FeCo nanocrystals with graphene layers by direct carbonization of $Fe_3[Co(CN)_6]_2$ spheres. Reproduced from Ref. 79 with permission from The Royal Society of Chemistry.

Table 7 Summary of the functionalized/modified graphene material-stabilized metal NPs and graphene material-supported surface-modified/protected metal NPs.

Metal	Stabilizer or Carrier System	Reductant 1	Catalysant/Substrate	Reductant 2	Solvent	Reaction Condition	Ref.
Ag	GO, PVP	glucose	4NP	$NaBH_4$	water	room temperature	87
Au	N-functionalized GSs using bromoacetonitrile as N source	electrochemical exfoliation of graphite followed by N functionaliation, trisodium citrate dihydrate, microwave-assisted	benzaldehyde	$NaBH_4$	water	room temperature, continuous stirring	196
FeCo	nitrogen doped graphene	carbonization of $Fe_3[Co(CN)_6]_2$ powders under a nitrogen flow at 900 °C	4NP	$NaBH_4$	water	room temperature	79
Au	GO, RGO, 2-mercaptopyridine	trisodium citrate	*o*-nitroaniline	$NaBH_4$	water	stirred at room temperature	195
Au	GO-Fe_3O_4 nanocomposite, 3-aminopropyltriethoxysilane	trisodium citrate, glucose	4NP	$NaBH_4$	water	room temperature	193
Au	tetraoctylammonium bromide, 4-dimethylaminopyridine, GO	$NaBH_4$	a series of nitroarenes	$NaBH_4$	water	room temperature, stirring	194
Au	ethanediamine-grafted GO	modified GO linked with Cu^+ (for seed), sodium formate (for growth)	4NP	$NaBH_4$	water	room temperature	192
Ag	RGO, tin(IV) prophyrin	phtotcatalytic processing to reduce both GO and Ag^+	4NP	$NaBH_4$	water	room temperature, sonication	198
Au	GO, tannic acid	tannic acid	4NP	$NaBH_4$	water	room temperature	82

2.6. Conclusion

In summary, schematic structural models, along with the corresponding description, of typical metal-based catalysts with different kinds of stabilizing systems are presented in Fig. 9. The structural features of these catalysts can be clearly revealed by the models.

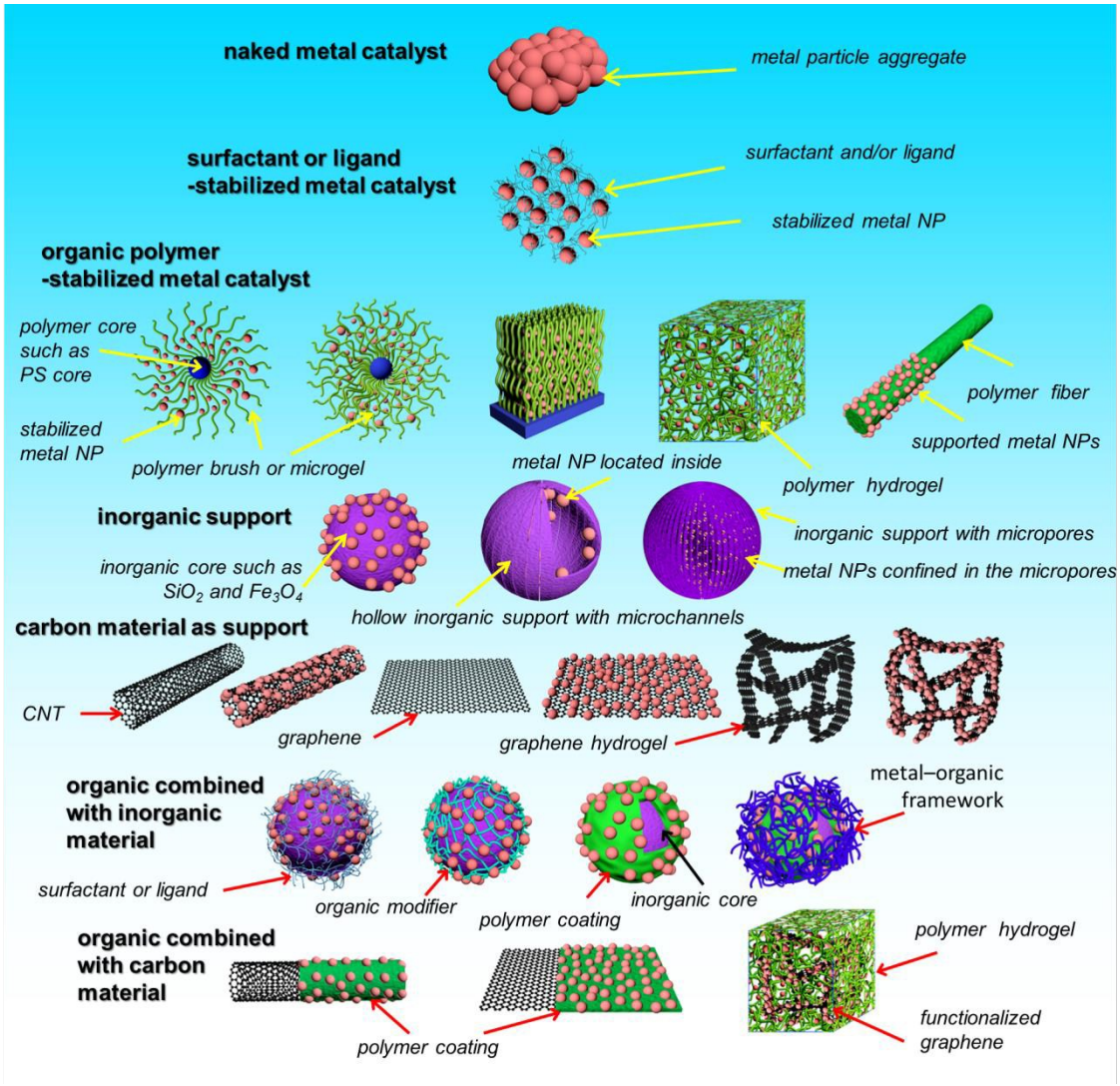

Fig. 9 Schematic structural models together with the corresponding description of the typical metal-based catalysts (with different kinds of stabilizing systems).

2.7. Remaining problems

(1) As discussed during the literature survey and also presented in Table 1-Table 7, most of the metal-based catalysts for aromatic pollutant reduction rely on scarcest precious

metals (e.g., Au, Pt, Pd and Ag). It is therefore highly desirable to explore more kinds of highly efficient and durable non-noble metal based catalysts for the reduction reactions in order to save the scarce metal resources, to slash the production cost, and to promote the possibility of large-scale applications.

(2) The studies summarized in the literature review have shown that single component-stabilized metal catalysts are less likely to achieve sufficient efficiency and durability for practical applications. It is therefore necessary to put more effort on rational design and fabrication of the integrated heterogeneous system with multiple functional components.

(3) As compared to the work involving use of surfactants, ligands, polymers, SiO_2 and Fe_3O_4 to stabilize metal catalysts for the reduction of aromatic pollutants (Table 3, Table 4, and Table 6), less work has been devoted to exploration of graphene materials as the metal catalyst supports despite the progress to date. Considering that the extraordinary physical and chemical properties of graphene materials can be exploited for design and fabrication of high-performance graphene-based composite catalysts, much work remains to be done in terms of sufficiently exploiting the extraordinary properties of graphene materials to fabricate high-performance composite catalysts.

(4) As pointed out during the literature review, much work did not consider the durability test of the catalysts explored, focusing only on the initial or fresh catalytic activity. This is an obvious shortage since the recyclability and reusability of the catalyst is equally important to its activity, especially for the heterogeneous catalyst. The ignored reusability test might also reveal that: (i) it is difficult to recycle the catalyst;

(ii) the reusability of the catalyst is unsatisfactory; (iii) the structure of the catalyst might be destructed or greatly changed during the catalytic reaction, especially under violent reaction condition with $NaBH_4$ as a reducing agent that is commonly used in the catalytic reduction of aromatic pollutants, as verified in Table 1-Table 7.

(5) Concerning the structural design for preparation of the metal NPs supported by a carrier system, many previous studies paid little attention to the importance of the binding species on the carrier system. Only dispersing of the metal NPs onto the carrier system without effective binding interactions usually cannot allow the stabilization of the metal NPs and formation of a durable composite catalyst even though weak van der Walls interactions may enable the metal NPs to be temporarily lodged on the carrier system. This indicates that some reported composite catalysts with metal NPs might be rather unstable and un-reusable because the metal NPs can suffer from an easy aggregation or leaching problem.

(6) Although an amount of work has attempted to fabricate high-performance metal-based catalysts, it is still difficult and challenging to achieve both the high activity and durability in a catalyst for the catalytic reduction reaction. Improving one property was always at the expense of the other. For instance, strong blocking or coordination of the metal nanocatalyst surfaces by organic surfactants or chelating agents can render the catalyst stable, whereas the catalytic activity is simultaneously compromised. Therefore, it is difficult but highly desirable for design and fabrication of the metal-based catalysts with both high activity and durability.

(7) In spite of some reported state-of-the-art catalysts possessing delicate structural features such as beautiful shape of metal NPs and elaborate assembly structures, their

preparation processes were usually time-consuming, complex, laborious and costly, with multistep procedures and a variety of raw materials involved, which limited the practical applications. Moreover, such beautifully structured metal-based catalysts cannot be more active and durable than the catalyst prepared by a much simpler, greener and lower-cost method, indicating that it is usually not necessary to laboriously fabricate an exquisite but inferior metal-based catalyst, especially from the viewpoint of practical application. This also reveals that it is highly desirable to explore highly efficient and durable metal-based composite catalysts using facile, inexpensive, relatively green, and efficient routes.

3. Conclusion

In this review article, we have systematically summarized the work devoted to fabrication and stabilization of metal-based catalysts for the reduction of water-soluble aromatic pollutants with focus on commonly used aromatic dye and nitro compounds, in order to address the issue of little attention paid to the review studies on this hot research area. The present review article categorizes the metal-based catalysts into different groups based on the stabilizing systems employed for synthesizing the metal catalyst. In addition to the catalytic reduction technique, other kinds of methods have also been briefly introduced such as adsorption and photocatalytic oxidation. While reviewing the studies on metal-based catalysts for the reduction reactions, the problems and aspects that might not be taken into account in the reports have been described. The remaining problems based on the literature survey have also been summarized at the end. As a result, the review paper presented here can shed light on future rational design and fabrication of

novel, low-cost, and highly efficient and durable metal-based catalysts for the hydrogenation reactions. The study will also provide impetus for future investigation on the high-performance composite catalyst containing a metal center through judicious integration of different components into a well-structured and high-performance composite. Furthermore, graphene materials used as the metal catalyst support are specifically reviewed and analyzed, which will pave the way for production of the high-performance graphene-based composite materials with metal nanocrystals for various applications, especially in catalysis, on the basis of the progress summarized.

Acknowledgement

This work was supported by the funding from Research Grants Council (RGC) of the Hong Kong SAR Government (funding code: PolyU 5316/10E).

References

1. B. K. Ghosh, S. Hazra, B. Naik and N. N. Ghosh, *Powder Technol.*, 2015, **269**, 371-378.
2. E. Clarke and R. Anliker, *Organic dyes and pigments: the handbook of environmental chemistry. Hutzinger*, Springer-Verlag, Heidelberg, 1980.
3. J. Hu, Y.-l. Dong, Z. u. Rahman, Y.-h. Ma, C.-l. Ren and X.-g. Chen, *Chem. Eng. J.*, 2014, **254**, 514-523.
4. Q. H. Hu, S. Z. Qiao, F. Haghseresht, M. A. Wilson and G. Q. Lu, *Ind. Eng. Chem. Res.*, 2006, **45**, 733-738.
5. V. K. Gupta and Suhas, *J. Environ. Manage.*, 2009, **90**, 2313-2342.
6. U. Pagga, *Water Res.*, 1994, **28**, 1051-1057.
7. M. Chen, P. Liu, C. Wang, W. Ren and G. Diao, *New J. Chem.*, 2014, **38**, 4566-4573.
8. Y. Xiong and H. T. Karlsson, *J. Environ. Health Part A*, 2001, **36**, 321-331.
9. N. H. Kalwar, Sirajuddin, S. T. H. Sherazi, A. R. Khaskheli, K. R. Hallam, T. B. Scott, Z. A. Tagar, S. S. Hassan and R. A. Soomro, *Appl. Catal. A: Gen.*, 2013, **453**, 54-59.
10. F. Liu, S. Chung, G. Oh and T. S. Seo, *ACS Appl. Mater. Interfaces*, 2012, **4**, 922-927.

11. L. Ai and J. Jiang, *Chem. Eng. J.*, 2012, **192**, 156-163.
12. G. K. Ramesha, A. Vijaya Kumara, H. B. Muralidhara and S. Sampath, *J. Colloid Interface Sci.*, 2011, **361**, 270-277.
13. V. H. Luan, J. S. Chung, E. J. Kim and S. H. Hur, *Chem. Eng. J.*, 2014, **246**, 64-70.
14. G. Annadurai, R. Juang and D. Lee, *J. Hazard. Mater.*, 2002, **92**, 263-274.
15. X. Wang, J. Ding, S. Yao, X. Wu, Q. Feng, Z. Wang and B. Geng, *J. Mater. Chem. A*, 2014, **2**, 15958-15963.
16. L.-M. Zhang, Y.-J. Zhou and Y. Wang, *J. Chem. Technol. Biotechnol.*, 2006, **81**, 799-804.
17. Y. Liu, Y. Zheng and A. Wang, *J. Environ. Sci.*, 2010, **22**, 486-493.
18. J. Fan, Z. Shi, M. Lian, H. Li and J. Yin, *J. Mater. Chem. A*, 2013, **1**, 7433-7443.
19. T. Wu, X. Cai, S. Tan, H. Li, J. Liu and W. Yang, *Chem. Eng. J.*, 2011, **173**, 144-149.
20. D. Liu, W. Lei, S. Qin and Y. Chen, *Sci. Rep.*, 2014, **4**, 4453-4451-4453-4455.
21. H. P. C. van Kuringen, G. M. Eikelboom, I. K. Shishmanova, D. J. Broer and A. P. H. J. Schenning, *Adv. Funct. Mater.*, 2014, **24**, 5045-5051.
22. C. Shen, Y. Shen, Y. Wen, H. Wang and W. Liu, *Water Res.*, 2011, **45**, 5200-5210.
23. M. Z. Iqbal and A. A. Abdala, *RSC Adv.*, 2013, **3**, 24455-24464.
24. X. Liu, L. Yan, W. Yin, L. Zhou, G. Tian, J. Shi, Z. Yang, D. Xiao, Z. Gu and Y. Zhao, *J. Mater. Chem. A*, 2014, **2**, 12296-12303.
25. H. Gao, Y. Sun, J. Zhou, R. Xu and H. Duan, *ACS Appl. Mater. Interfaces*, 2013, **5**, 425-432.
26. W. Zhou, T. Li, J. Wang, Y. Qu, K. Pan, Y. Xie, G. Tian, L. Wang, Z. Ren, B. Jiang and H. Fu, *Nano Res.*, 2014, **7**, 731-742.
27. U. T. D. Thuy, N. Q. Liem, C. M. A. Parlett, G. M. Lalev and K. Wilson, *Catal. Commun.*, 2014, **44**, 62-67.
28. C. Feng, H. Shang and X. Liu, *Chinese J. Catal.*, 2014, **35**, 168-174.
29. A. A. Aziz, C. K. Cheng, S. Ibrahim, M. Matheswaran and P. Saravanan, *Chem. Eng. J.*, 2012, **183**, 349-356.
30. R. A. Soomro, S. T. H. Sherazi, N. M. Sirajuddin, M. Raza, N. H. K. Shah, K. R. Hallam and A. Shah, *Adv. Mat. Lett.* , 2014, **5**, 191-198.
31. A. Biffis, M. Zecca and M. Basato, *Eur. J. Inorg. Chem.*, 2001, **2001**, 1131-1133.
32. D. H. Atha, H. Wang, E. J. Petersen, D. Cleveland, R. D. Holbrook, P. Jaruga, M. Dizdaroglu, B. Xing and B. C. Nelson, *Environ. Sci. Technol.*, 2012, **46**, 1819-1827.
33. H.-W. Hu, J. H. Xin and H. Hu, *ChemPlusChem*, 2013, **78**, 1483-1490.
34. K. S. Kim, Y. Zhao, H. Jang, S. Y. Lee, J. M. Kim, K. S. Kim, J.-H. Ahn, P. Kim, J.-Y. Choi and B. H. Hong, *Nature*, 2009, **457**, 706-710.
35. K. S. Novoselov, A. K. Geim, S. V. Morozov, D. Jiang, Y. Zhang, S. V. Dubonos, I. V. Grigorieva and A. A. Firsov, *Science*, 2004, **306**, 666-669.
36. K. R. Reddy, M. Hassan and V. G. Gomes, *Appl. Catal. A: Gen.*, 2015, **489**, 1-16.
37. Y. Liang, H. Wang, H. Sanchez Casalongue, Z. Chen and H. Dai, *Nano Res.*, 2010, **3**, 701-705.

38. Q.-P. Luo, X.-Y. Yu, B.-X. Lei, H.-Y. Chen, D.-B. Kuang and C.-Y. Su, *J. Phys. Chem. C*, 2012, **116**, 8111-8117.
39. A. Ye, W. Fan, Q. Zhang, W. Deng and Y. Wang, *Catal. Sci. Technol.*, 2012, **2**, 969-978.
40. X. An, J. C. Yu and J. Tang, *J. Mater. Chem. A*, 2014, **2**, 1000-1005.
41. X.-Y. Zhang, H.-P. Li, X.-L. Cui and Y. Lin, *J. Mater. Chem.*, 2010, **20**, 2801-2806.
42. J. Liu, H. Bai, Y. Wang, Z. Liu, X. Zhang and D. D. Sun, *Adv. Funct. Mater.*, 2010, **20**, 4175-4181.
43. T. Xu, L. Zhang, H. Cheng and Y. Zhu, *Appl. Catal. B*, 2011, **101**, 382-387.
44. U. P. Azad, V. Ganesan and M. Pal, *J. Nanopart. Res.*, 2011, **13**, 3951-3959.
45. Z.-J. Jiang, C.-Y. Liu and L.-W. Sun, *J. Phys. Chem. B*, 2005, **109**, 1730-1735.
46. W. Wang, F. Wang, Y. Kang and A. Wang, *Chem. Eng. J.*, 2014, **237**, 336-343.
47. J. Li, C.-y. Liu and Y. Liu, *J. Mater. Chem.*, 2012, **22**, 8426-8430.
48. Y. Zheng and A. Wang, *J. Mater. Chem.*, 2012, **22**, 16552-16559.
49. H. Hu, J. H. Xin and H. Hu, *J. Mater. Chem. A*, 2014, **2**, 11319-11333.
50. Y. Junejo, Sirajuddin, A. Baykal, M. Safdar and A. Balouch, *Appl. Surf. Sci.*, 2014, **290**, 499-503.
51. Z. Deng, M. Chen and L. Wu, *J. Phys. Chem. C*, 2007, **111**, 11692-11698.
52. C. Wen, M. Shao, S. Zhuo, Z. Lin and Z. Kang, *Mater. Chem. Phys.*, 2012, **135**, 780-785.
53. A. Amarjargal, L. D. Tijing, I.-T. Im and C. S. Kim, *Chem. Eng. J.*, 2013, **226**, 243-254.
54. S. S. Hassan, Sirajuddin, A. R. Solangi, M. H. Agheem, Y. Junejo, N. H. Kalwar and Z. A. Tagar, *J. Hazard. Mater.*, 2011, **190**, 1030-1036.
55. R. Dong, J. Xu, Z. Yang, G. Wei, W. Zhao, J. Yan, Y. Fang and J. Hao, *Chem. Eur. J.*, 2013, **19**, 13099-13104.
56. M. Tang, S. Zhang, X. Li, X. Pang and H. Qiu, *Mater. Chem. Phys.*, 2014, **148**, 639-647.
57. Y. Zhang, P. Zhu, L. Chen, G. Li, F. Zhou, D. Lu, R. Sun, F. Zhou and C.-p. Wong, *J. Mater. Chem. A*, 2014, **2**, 11966-11973.
58. R. Kuttiplavil Narayanan, S. Janardanan Devaki and T. Prasada Rao, *Appl. Catal. A: Gen.*, 2014, **483**, 31-40.
59. G. P. Sahoo, D. Kumar Bhui, D. Das and A. Misra, *J. Mol. Liq.*, 2014, **198**, 215-222.
60. V. K. Gupta, N. Atar, M. L. Yola, Z. Üstündağ and L. Uzun, *Water Res.*, 2014, **48**, 210-217.
61. P. Zhang, C. Shao, Z. Zhang, M. Zhang, J. Mu, Z. Guo and Y. Liu, *Nanoscale*, 2011, **3**, 3357-3363.
62. Y. Lu, Y. Mei, M. Drechsler and M. Ballauff, *Angew. Chem. Int. Ed.*, 2006, **45**, 813-816.
63. Y. Shin, A. Dohnalkova and Y. Lin, *J. Phys. Chem. C*, 2010, **114**, 5985-5989.
64. S. Harish, J. Mathiyarasu, K. L. N. Phani and V. Yegnaraman, *Catal. Lett.*, 2008, **128**, 197-202.
65. H. Liu and Q. Yang, *J. Mater. Chem.*, 2011, **21**, 11961-11967.

66. S.-D. Oh, M.-R. Kim, S.-H. Choi, J.-H. Chun, K.-P. Lee, A. Gopalan, C.-G. Hwang, K. Sang-Ho and O. J. Hoon, *J. Ind. Eng. Chem.*, 2008, **14**, 687-692.
67. T. Yao, T. Cui, X. Fang, F. Cui and J. Wu, *Nanoscale*, 2013, **5**, 5896-5904.
68. S. Tang, S. Vongehr and X. Meng, *J. Mater. Chem.*, 2010, **20**, 5436-5445.
69. C. Pearce, *Dyes and Pigments*, 2003, **58**, 179-196.
70. S. Wunder, F. Polzer, Y. Lu, Y. Mei and M. Ballauff, *J. Phys. Chem. C*, 2010, **114**, 8814-8820.
71. B. Ballarin, M. C. Cassani, D. Tonelli, E. Boanini, S. Albonetti, M. Blosi and M. Gazzano, *J. Phys. Chem. C*, 2010, **114**, 9693-9701.
72. Z. Wang, H. Fu, D. Han and F. Gu, *J. Mater. Chem. A*, 2014, **2**, 20374-20381.
73. J. You, C. Zhao, J. Cao, J. Zhou and L. Zhang, *J. Mater. Chem. A*, 2014, **2**, 8491-8499.
74. M. Horecha, E. Kaul, A. Horechyy and M. Stamm, *J. Mater. Chem. A*, 2014, **2**, 7431-7438.
75. Z. Dong, X. Le, Y. Liu, C. Dong and J. Ma, *J. Mater. Chem. A*, 2014, **2**, 18775-18785.
76. P. Yang, A.-D. Xu, J. Xia, J. He, H.-L. Xing, X.-M. Zhang, S.-Y. Wei and N.-N. Wang, *Appl. Catal. A: Gen.*, 2014, **470**, 89-96.
77. J.-J. Lv, A.-J. Wang, X. Ma, R.-Y. Xiang, J.-R. Chen and J.-J. Feng, *J. Mater. Chem. A*, 2015, **3**, 290-296.
78. V. Vetere, A. B. Merlo and M. L. Casella, *Appl. Catal. A: Gen.*, 2015, **491**, 70-77.
79. L. Hu, R. Zhang, L. Wei, F. Zhang and Q. Chen, *Nanoscale*, 2015, **7**, 450-454.
80. M. S. Holden, K. E. Nick, M. Hall, J. R. Milligan, Q. Chen and C. C. Perry, *RSC Adv.*, 2014, **4**, 52279-52288.
81. Z. Zhang, C. Shao, P. Zou, P. Zhang, M. Zhang, J. Mu, Z. Guo, X. Li, C. Wang and Y. Liu, *Chem. Commun.*, 2011, **47**, 3906-3908.
82. Y. Zhang, S. Liu, W. Lu, L. Wang, J. Tian and X. Sun, *Catal. Sci. Technol.*, 2011, **1**, 1142-1144.
83. H. Li, J. Liao, Y. Du, T. You, W. Liao and L. Wen, *Chem. Commun.*, 2013, **49**, 1768-1770.
84. M. Li and G. Chen, *Nanoscale*, 2013, **5**, 11919-11927.
85. C.-H. Kuo, T.-F. Chiang, L.-J. Chen and M. H. Huang, *Langmuir*, 2004, **20**, 7820-7824.
86. X. Zhou, X. Huang, X. Qi, S. Wu, C. Xue, F. Y. C. Boey, Q. Yan, P. Chen and H. Zhang, *J. Phys. Chem. C*, 2009, **113**, 10842-10846.
87. C. Xu and X. Wang, *Colloids Surf. A*, 2012, **404**, 78-82.
88. M. Blosi, S. Albonetti, M. Dondi, C. Martelli and G. Baldi, *J. Nanopart. Res.*, 2010, **13**, 127-138.
89. E. Filippo, A. Serra and D. Manno, *Sensors Actuators B: Chem.*, 2009, **138**, 625-630.
90. G. P. Sahoo, S. Basu, S. Samanta and A. Misra, *J. Exp. Nanosci.*, 2014, DOI: 10.1080/17458080.2013.877163, 1-13.
91. I. Washio, Y. Xiong, Y. Yin and Y. Xia, *Adv. Mater.*, 2006, **18**, 1745-1749.
92. V. R. Chaudhari, K. M. Samant, P. P. Ingole, P. A. Hassan and S. K. Haram, *Int. J. Nanotechnol.*, 2011, **8**, 988-997.

93. W. C. Elias, R. Eising, T. R. Silva, B. L. Albuquerque, E. Martendal, L. Meier and J. B. Domingos, *J. Phys. Chem. C*, 2014, **118**, 12962-12971.
94. C. Huang, C. Chen, X. Ye, W. Ye, J. Hu, C. Xu and X. Qiu, *J. Mater. Chem. A*, 2013, **1**, 12192-12197.
95. T. Sinha, M. Ahmaruzzaman, A. Bhattacharjee, M. Asif and V. K. Gupta, *J. Mol. Liq.*, 2015, **201**, 113-123.
96. L. Sun, J. He, S. An, J. Zhang, J. Zheng and D. Ren, *Chinese J. Catal.*, 2013, **34**, 1378-1385.
97. Y. Lu, Y. Mei, R. Walker, M. Ballauff and M. Drechsler, *Polymer*, 2006, **47**, 4985-4995.
98. Y. Mei, Y. Lu, F. Polzer, M. Ballauff and M. Drechsler, *Chem. Mater.*, 2007, **19**, 1062-1069.
99. Y. Lu, Y. Mei, M. Ballauff and M. Drechsler, *J. Phys. Chem. B*, 2006, **110**, 3930-3937.
100. Y. Lu, P. Spyra, Y. Mei, M. Ballauff and A. Pich, *Macromol. Chem. Phys.*, 2007, **208**, 254-261.
101. M. Kumar, L. Varshney and S. Francis, *Radiat. Phys. Chem.*, 2005, **73**, 21-27.
102. M. F. Ottaviani, R. Valluzzi and L. Balogh, *Macromolecules*, 2002, **35**, 5105-5115.
103. Z. Liu, X. Wang, H. Wu and C. Li, *J. Colloid Interface Sci.*, 2005, **287**, 604-611.
104. S. Fazzini, D. Nanni, B. Ballarin, M. C. Cassani, M. Giorgetti, C. Maccato, A. Trapananti, G. Aquilanti and S. I. Ahmed, *J. Phys. Chem. C*, 2012, **116**, 25434-25443.
105. K. Esumi, K. Miyamoto and T. Yoshimura, *J. Colloid Interface Sci.*, 2002, **254**, 402-405.
106. K. Hayakawa, T. Yoshimura and K. Esumi, *Langmuir*, 2003, **19**, 5517-5521.
107. E. O. Pentsak, E. G. Gordeev and V. P. Ananikov, *ACS Catal.*, 2014, **4**, 3806-3814.
108. S. Stankovich, D. A. Dikin, G. H. B. Dommett, K. M. Kohlhaas, E. J. Zimney, E. A. Stach, R. D. Piner, S. T. Nguyen and R. S. Ruoff, *Nature*, 2006, **442**, 282-286.
109. H. Hu, C. C. K. Allan, J. Li, Y. Kong, X. Wang, J. H. Xin and H. Hu, *Nano Res.*, 2014, **7**, 418-433.
110. H. Hu, J. H. Xin, H. Hu, A. Chan and L. He, *Carbohydr. Polym.*, 2013, **91**, 305-313.
111. H.-W. Hu, G.-H. Chen, M. Fang and W.-F. Zhao, *Synth. Met.*, 2009, **159**, 1505-1507.
112. H. Hu and G. Chen, *Polym. Compos.*, 2010, **31**, 1770-1775.
113. H. Hu, L. Chen and G. Chen, *Mater. Manuf. Processes*, 2011, **26**, 618-622.
114. B. P. Tripathi and V. K. Shahi, *Prog. Polym. Sci.*, 2011, **36**, 945-979.
115. W. Li, F. Xia, J. Qu, P. Li, D. Chen, Z. Chen, Y. Yu, Y. Lu, R. A. Caruso and W. Song, *Nano Res.*, 2014, **7**, 903-916.
116. H. Li, L. Han, J. Cooper-White and I. Kim, *Green Chem.*, 2012, **14**, 586-591.
117. I. V. Lightcap, T. H. Kosel and P. V. Kamat, *Nano Lett.*, 2010, **10**, 577-583.
118. K. M. Samant, V. R. Chaudhari, S. Kapoor and S. K. Haram, *Carbon*, 2007, **45**, 2126-2129.

119. H. Hu, J. H. Xin, H. Hu, X. Wang and Y. Kong, *Appl. Catal. A: Gen.*, 2015, **492**, 1-9.
120. H. Hu, J. Xin, H. Hu, X. Wang and X. Lu, *Molecules*, 2014, **19**, 7459-7479.
121. H. A. Elazab, A. R. Siamaki, S. Moussa, B. F. Gupton and M. S. El-Shall, *Appl. Catal. A: Gen.*, 2015, **491**, 58-69.
122. K. S. Hui, K. N. Hui, D. A. Dinh, C. H. Tsang, Y. R. Cho, W. Zhou, X. Hong and H.-H. Chun, *Acta Mater.*, 2014, **64**, 326-332.
123. G. M. Scheuermann, L. Rumi, P. Steurer, W. Bannwarth and R. Mülhaupt, *J. Am. Chem. Soc.*, 2009, **131**, 8262-8270.
124. Y. Qu and X. Duan, *Chem. Soc. Rev.*, 2013, **42**, 2568-2580.
125. V. I. Isaeva, M. I. Barkova, L. Kustov, D. A. Syrtsova, E. Efimova and V. Teplyakov, *J. Mater. Chem. A*, 2015, DOI: 10.1039/c5ta01178g.
126. W. Long, N. A. Brunelli, S. A. Didas, E. W. Ping and C. W. Jones, *ACS Catal.*, 2013, **3**, 1700-1708.
127. Y. Du, H. Chen, R. Chen and N. Xu, *Appl. Catal. A: Gen.*, 2004, **277**, 259-264.
128. R. Chen, Q. Wang, Y. Du, W. Xing and N. Xu, *Chem. Eng. J.*, 2009, **145**, 371-376.
129. J. Huang, S. Vongehr, S. Tang, H. Lu, J. Shen and X. Meng, *Langmuir*, 2009, **25**, 11890-11896.
130. J. Huang, S. Vongehr, S. Tang, H. Lu and X. Meng, *J. Phys. Chem. C*, 2010, **114**, 15005-15010.
131. N. Pradhan, A. Pal and T. Pal, *Colloids Surf. A*, 2002, **196**, 247-257.
132. S. Tang, S. Vongehr, Y. Wang, J. Cui, X. Wang and X. Meng, *J. Mater. Chem. A*, 2014, **2**, 3648-3660.
133. X. Yang, H. Zhong, Y. Zhu, H. Jiang, J. Shen, J. Huang and C. Li, *J. Mater. Chem. A*, 2014, **2**, 9040-9047.
134. N. B. Golovina and L. M. Kustov, *Mendeleev Commun.*, 2013, **23**, 59-65.
135. D. Jiang, J. Xie, M. Chen, D. Li, J. Zhu and H. Qin, *J. Alloys Compd.*, 2011, **509**, 1975-1979.
136. R. Chadha, A. Das, N. Maiti and S. Kapoor, *Mater. Chem. Phys.*, 2014, **148**, 1124-1130.
137. S. Kundu, S. Lau and H. Liang, *J. Phys. Chem. C*, 2009, **113**, 5150-5156.
138. S. Kundu, K. Wang and H. Liang, *J. Phys. Chem. C*, 2009, **113**, 18570-18577.
139. S. Kundu and H. Liang, *J. Colloid Interface Sci.*, 2011, **354**, 597-606.
140. R. Narayanan and M. A. El-Sayed, *J. Am. Chem. Soc.*, 2004, **126**, 7194-7195.
141. R. Eising, W. C. Elias, B. L. Albuquerque, S. Fort and J. B. Domingos, *Langmuir*, 2014, **30**, 6011-6020.
142. M. Meenakumari and D. Philip, *Spectrochim. Acta A*, 2015, **135**, 632-638.
143. H. P. Borase, C. D. Patil, R. B. Salunkhe, R. K. Suryawanshi, B. K. Salunke and S. V. Patil, *Bioprocess Biosyst. Eng.*, 2014, **37**, 1695-1705.
144. Y. Junejo and A. Baykal, *Turk. J. Chem.*, 2014, **38**, 765-774.
145. M. Priebe and K. M. Fromm, *Part. Part. Syst. Charact.*, 2014, **31**, 645-651.
146. Y. Sun, F. Zhang, L. Xu, Z. Yin and X. Song, *J. Mater. Chem. A*, 2014, **2**, 18583-18592.
147. M. Meena Kumari, J. Jacob and D. Philip, *Spectrochim. Acta A*, 2015, **137**, 185-192.

148. Y. Junejo, A. Güner and A. Baykal, *Appl. Surf. Sci.*, 2014, **317**, 914-922.
149. Y. Junejo, A. Baykal and Sirajuddin, *Journal of Inorganic and Organometallic Polymers and Materials*, 2013, **24**, 401-406.
150. P. Zhang, Y. Sui, C. Wang, Y. Wang, G. Cui, C. Wang, B. Liu and B. Zou, *Nanoscale*, 2014, **6**, 5343-5350.
151. L. Ai and J. Jiang, *Bioresour. Technol.*, 2013, **132**, 374-377.
152. M. Ajmal, M. Siddiq, H. Al-Lohedan and N. Sahiner, *RSC Adv.*, 2014, **4**, 59562-59570.
153. N. Sahiner, S. Yildiz and H. Al-Lohedan, *Appl. Catal. B*, 2015, **166-167**, 145-154.
154. S. Saha, A. Pal, S. Kundu, S. Basu and T. Pal, *Langmuir*, 2010, **26**, 2885-2893.
155. K. Esumi, R. Isono and T. Yoshimura, *Langmuir*, 2004, **20**, 237-243.
156. Q. B. Yang, D. M. Li, Y. L. Hong, Z. Y. Li, C. Wang, S. L. Qiu and Y. Wei, *Synth. Met.*, 2003, **137**, 973-974.
157. C. Zhang, Q. Yang, N. Zhan, L. Sun, H. Wang, Y. Song and Y. Li, *Colloids Surf. A*, 2010, **362**, 58-64.
158. T. Yao, T. Cui, H. Wang, L. Xu, F. Cui and J. Wu, *Nanoscale*, 2014, **6**, 7666-7674
159. M. Li, V. Zhong and G. Chen, *MRS Proceedings*, 2014, **1641**, 1-9.
160. S. Panigrahi, S. Basu, S. Praharaj, S. Pande, S. Jana, A. Pal, S. K. Ghosh and T. Pal, *J. Phys. Chem. C*, 2007, **111**, 4596-4605.
161. A. G. Majouga, E. K. Beloglazkina, E. A. Manzheliy, D. A. Denisov, E. G. Evtushenko, K. I. Maslakov, E. V. Golubina and N. V. Zyk, *Appl. Surf. Sci.*, 2015, **325**, 73-78.
162. Z. Deng, H. Zhu, B. Peng, H. Chen, Y. Sun, X. Gang, P. Jin and J. Wang, *ACS Appl. Mater. Interfaces*, 2012, **4**, 5625-5632.
163. A. C. Patel, S. Li, C. Wang, W. Zhang and Y. Wei, *Chem. Mater.*, 2007, **19**, 1231-1238.
164. J. Zheng, Y. Dong, W. Wang, Y. Ma, J. Hu, X. Chen and X. Chen, *Nanoscale*, 2013, **5**, 4894-4901.
165. E. V. Starodubtseva, M. G. Vinogradov, O. V. Turova, N. A. Bumagin, E. G. Rakov and V. I. Sokolov, *Catal. Commun.*, 2009, **10**, 1441-1442.
166. M. A. Ryashentseva, E. V. Egorova, A. I. Trusov, E. R. Nougmanov and S. N. Antonyuk, *Russian Chemical Reviews*, 2006, **75**, 1003-1014.
167. H. He and C. Gao, *J. Nanomater.*, 2011, **2011**, 1-10.
168. M. L. Kantam, R. Chakravarti, U. Pal, B. Sreedhar and S. Bhargava, *Adv. Synth. Catal.*, 2008, **350**, 822-827.
169. R. Chen, Y. Du, W. Xing and N. Xu, *Chin. J. Chem. Eng.*, 2007, **15**, 884-888.
170. P. L. Gkizis, M. Stratakis and I. N. Lykakis, *Catal. Commun.*, 2013, **36**, 48-51.
171. M. J. Vaidya, S. M. Kulkarni and R. V. Chaudhari, *Org. Process Res. Dev.*, 2003, **7**, 202-208.
172. R. Nie, J. Wang, L. Wang, Y. Qin, P. Chen and Z. Hou, *Carbon*, 2012, **50**, 586-596.
173. L. Guardia, S. Villar-Rodil, J. I. Paredes, R. Rozada, A. Martínez-Alonso and J. M. D. Tascón, *Carbon*, 2012, **50**, 1014-1024.
174. B. K. Barman and K. K. Nanda, *Chem. Commun.*, 2013, **49**, 8949-8951.
175. B. K. Barman and K. K. Nanda, *Appl. Catal. A: Gen.*, 2015, **491**, 45-51.

176. T. Som, G. V. Troppenz, R. Wendt, M. Wollgarten, J. Rappich, F. Emmerling and K. Rademann, *ChemSusChem*, 2014, **7**, 854-865.
177. R. S. Sai Siddhardha, V. Lakshman Kumar, A. Kaniyoor, V. Sai Muthukumar, S. Ramaprabhu, R. Podila, A. M. Rao and S. S. Ramamurthy, *Spectrochim. Acta A*, 2014, **133**, 365-371.
178. H. He and C. Gao, *Sci. China Chem.*, 2011, **54**, 397-404.
179. K. S. Rao, J. Sentilnathan, H.-W. Cho, J.-J. Wu and M. Yoshimura, *Adv. Funct. Mater.*, 2015, **25**, 298-305.
180. L. Tzounis, R. Contreras-Caceres, L. Schellkopf, D. Jehnichen, D. Fischer, C. Cai, P. Uhlmann and M. Stamm, *RSC Adv.*, 2014, **4**, 17846-17855.
181. L. Q. Xu, B. S. M. Yap, R. Wang, K.-G. Neoh, E.-T. Kang and G. D. Fu, *Ind. Eng. Chem. Res.*, 2014, **53**, 3116-3124.
182. Y.-C. Chang and D.-H. Chen, *J. Hazard. Mater.*, 2009, **165**, 664-669.
183. K. Jiang, H.-X. Zhang, Y.-Y. Yang, R. Mothes, H. Lang and W.-B. Cai, *Chem. Commun.*, 2011, **47**, 11924-11926.
184. F.-h. Lin and R.-a. Doong, *J. Phys. Chem. C*, 2011, **115**, 6591-6598.
185. U. Kurtan and A. Baykal, *Mater. Res. Bull.*, 2014, **60**, 79-87.
186. F. Ke, L. Wang and J. Zhu, *Nanoscale*, 2015, **7**, 1201-1208.
187. A. Taketoshi and M. Haruta, *Chem. Lett.*, 2014, **43**, 380-387.
188. S. Ramalingam, L. B. Devi, J. Raghava Rao and B. Unni Nair, *RSC Adv.*, 2014, **4**, 56041-56051.
189. F. Ke, J. Zhu, L.-G. Qiu and X. Jiang, *Chem. Commun.*, 2013, **49**, 1267-1269.
190. A. Mignani, S. Fazzini, B. Ballarin, E. Boanini, M. C. Cassani, C. Maccato, D. Barreca and D. Nanni, *RSC Adv.*, 2015, **5**, 9600-9606.
191. S. Fazzini, M. C. Cassani, B. Ballarin, E. Boanini, J. S. Girardon, A.-S. Mamede, A. Mignani and D. Nanni, *J. Phys. Chem. C*, 2014, **118**, 24538-24547.
192. Y. Ju, X. Li, J. Feng, Y. Ma, J. Hu and X. Chen, *Appl. Surf. Sci.*, 2014, **316**, 132-140.
193. J. Hu, Y.-l. Dong, X.-j. Chen, H.-j. Zhang, J.-m. Zheng, Q. Wang and X.-g. Chen, *Chem. Eng. J.*, 2014, **236**, 1-8.
194. Y. Choi, H. S. Bae, E. Seo, S. Jang, K. H. Park and B.-S. Kim, *J. Mater. Chem.*, 2011, **21**, 15431-15436.
195. J. Huang, L. Zhang, B. Chen, N. Ji, F. Chen, Y. Zhang and Z. Zhang, *Nanoscale*, 2010, **2**, 2733-2738.
196. K. Sanjeeva Rao, J. Senthilnathan, J.-M. Ting and M. Yoshimura, *Nanoscale*, 2014, **6**, 12758-12768.
197. X.-k. Kong, Z.-y. Sun, M. Chen, C.-l. Chen and Q.-w. Chen, *Energ. Environ. Sci.*, 2013, **6**, 3260-3266.
198. H. Li, Y. Zhang, G. Chang, S. Liu, J. Tian, Y. Luo, A. M. Asiri, A. O. Al-Youbi and X. Sun, *ChemPlusChem*, 2012, **77**, 545-550.